land

MDPI

*Article*

# Assessing the Trade-Offs and Synergies Among Ecosystem Services Under Multiple Land-Use Scenarios in the Beijing–Tianjin–Hebei Region

**Xiaoru He [1], Yang Li [2], Wei Li [1,3,4,*], Zhijun Shen [1], Baoni Xie [1,3,4], Shuhui Yu [1,3,4], Shufei Wang [1], Nan Wang [5], Zhe Li [1], Jianxia Zhao [6], Yancang Li [1,3,4,*] and Shuqin Zhao [1]**

[1] School of Land Science and Space Planning, Hebei GEO University, Shijiazhuang 052161, China
[2] Center of Construction Management & Quality & Safety Supervision, Ministry of Water Resources, Beijing 100038, China
[3] International Science and Technology Cooperation Base of Hebei Province: Hebei International Joint Research Center for Remote Sensing of Agricultural Drought Monitoring, Hebei GEO University, Shijiazhuang 052161, China
[4] Field Scientific Observation and Research Station for Land Ecology and Land Use in Haihe River Basin, Shijiazhuang 050051, China
[5] Safety and Security Office, Yanshan University, Qinhuangdao 066004, China
[6] College of Geography and Land Engineering, Yuxi Normal University, Yuxi 653100, China
* Correspondence: weil87land@hgu.edu.cn (W.L.); liyancang@hebeu.edu.cn (Y.L.)

## Abstract

To enhance ecosystem services (ESs) benefits and promote ecological–economic–sociologic sustainability in highly urbanized regions such as the Beijing–Tianjin–Hebei (BTH) region, it is essential to assess the dynamic changes in ESs within these regions from a functional zoning perspective and to explore the interactions between ESs. This research delved into how ESs change over space and time, using land-use projections for 2035 based on Natural Development (ND), Ecological Protection (EP), Economic Construction (EC) scenarios. This study also took a close look at the interplay of these ESs across BTH and its five distinct functional zones: the Bashang Plateau Ecological Protection Zone (BS), the Northwestern Ecological Conservation Zone (ST), the Central Core Functional Zone (HX), the Southern Functional Expansion Zone (TZ), and the Eastern Coastal Development Zone (BH). We utilize the Multiple Ecosystem Service Landscape Index (MESLI) to assess the capacity to supply multiple ESs. Key results include the following: (1) Projected land-use changes for 2035 scenarios consistently show cropland and grassland declining, while forest and urbanland expand, though the magnitude of change varies by scenario. (2) Habitat quality, carbon storage, and soil conservation displayed a "high northwest–low southeast" gradient, opposite to water yield. The average MESLI value declined in all scenarios relative to 2020, with the highest value under the EP scenario. (3) Synergies prevailed between habitat quality, carbon storage, and soil conservation, while trade-offs occurred with water yield. These relationships varied spatially—for instance, habitat quality and soil conservation were weakly synergistic in the BS but showed weak trade-offs in the HX. These insights can inform management strategies in other rapidly urbanizing regions.

**Keywords:** functional zones; multi-scenario land-use change; ecosystem services (ESs); the Beijing–Tianjin–Hebei region; trade-offs and synergies

check for updates

Academic Editor: Alessandro Gimona

Received: 22 September 2025
Revised: 26 October 2025
Accepted: 30 October 2025
Published: 1 November 2025

**Citation:** He, X.; Li, Y.; Li, W.; Shen, Z.; Xie, B.; Yu, S.; Wang, S.; Wang, N.; Li, Z.; Zhao, J.; et al. Assessing the Trade-Offs and Synergies Among Ecosystem Services Under Multiple Land-Use Scenarios in the Beijing–Tianjin–Hebei Region. *Land* **2025**, *14*, 2176. https://doi.org/10.3390/land14112176

**Copyright:** © 2025 by the authors. Licensee MDPI, Basel, Switzerland. This article is an open access article distributed under the terms and conditions of the Creative Commons Attribution (CC BY) license (https://creativecommons.org/licenses/by/4.0/).

## 1. Introduction

Ecosystem services (ESs) are the natural conditions and functions of the environment maintained by ecosystems, providing direct and indirect benefits to human [1–4]. ESs are vital for sustaining regional ecological balance, fostering sustainable economic and social progress, and improving human health and happiness [5–7]. Nevertheless, given the diversity of human demands, spatial heterogeneity in land-use patterns, and complexity of ecological processes, ESs interact through complex nonlinear relationships, characterized by trade-offs (mutually offsetting effects) and synergies (reinforcing effects) [8,9]. Synergies occur when two ESs exhibit concurrent increases or decreases in their provision levels. Conversely, trade-offs denote an inverse relationship where enhancing one ES compromises another. Synergistic ESs interactions may significantly enhance ecological efficiency, including greenhouse gas reductions and climate change mitigation [10,11]. Since regions with high ecosystem service capacity often do not align with locations of human demand, when people attempt to maximize the benefits of a particular ecosystem service function, they simultaneously alter other ecosystem service functions. Implementing such targeted ecosystem management measures within a social–ecological system triggers internal cascading effects, thereby intensifying trade-offs between ESs [12,13]. Empirical studies indicate that failing to account for the trade-offs and synergies between ESs in land management strategies hinder ecosystem optimization and accelerate ecosystem degradation [14]. Consequently, comprehending how regional land-use alterations influence essential ESs and examining the intricate feedback interactions among them is vital to achieving a sustainable balance between anthropogenic demands and ecological gains in areas undergoing rapid urbanization.

Three primary methodologies are commonly employed to identify ESs relationships: statistical analyses, spatial mapping techniques, and scenario-based assessments. Statistical analysis methods primarily encompass regression models and multi-objective optimization frameworks, which numerous scholars have extensively employed to evaluate the interrelationships between ESs [15,16]. For instance, some researchers have effectively utilized correlation analysis to reveal dynamic relationships between ESs [17,18]. Spatial technologies enable the spatial representation of ESs. When combined with geospatial overlay tools, they can visually identify trade-off/synergy hotspots for ESs [19]. Nevertheless, most existing studies focus predominantly on current ESs interactions, while largely neglecting their dynamic evolution under alternative future scenarios. Scenario analysis represents the most established approach for projecting future ESs relationships [20]. Empirical studies confirm that land use/cover change (LUCC)—induced by socioeconomic transitions and urbanization—represent a key driver of ESs modifications [21–23]. Global modeling studies provide evidence that LUCC significantly alters precipitation patterns and atmospheric circulation through land–atmosphere interactions, thereby influencing local and regional climate conditions [24]. LUCC impacts biodiversity and species distribution by altering hydrological dynamics [25,26]. Additionally, the analysis indicates that the quantity, scale, and spatial pattern of distinct land-use types will vary considerably across different future development pathways [27]. These LUCC transformations will subsequently reshape ecosystem structures and processes, thereby modifying ESs functionality and their interdependencies [28,29]. Scholars have developed diverse land-use scenarios to analyze ESs dynamics, providing evidence-based recommendations for land-use planning [30,31]. Conventional land-use simulation frameworks (e.g., CLUE-S [32], CA-Markov [33], and FLUS [34]) exhibit limitations in capturing spatiotemporal patch dynamics and identifying change drivers [35]. However, the PLUS model [36] incorporates a Land Expansion Analysis Strategy (LEAS) and a mechanism for generating multi-type random patch seeds (CARS), achieving superior simulation accuracy while identifying change drivers. How-

ever, prevailing modeling practices often rely on uniform scenario assumptions that are applied indiscriminately across entire study areas [37,38]. This approach overlooks the inherent spatial variation in key drivers—such as topography, climatic factors, and regional planning policies—thereby limiting the realism and accuracy of land-use projections. This oversimplification undermines the precision of ecological management strategies [39,40]. Mounting evidence indicates that local factors (e.g., geomorphology and functional zoning) critically influence land-use allocation patterns [6,14], ultimately affecting the reliability of ESs assessments across scenarios. Neglecting such heterogeneity may compromise the credibility of ESs evaluations under different scenario projections. Studying the characteristics of ESs trade-offs and synergies under different future scenarios from a functional zoning perspective facilitates the balancing of regulating and provisioning services in key regions. Concurrently, it enables the formulation of differentiated ecological management measures based on specific zones and categories, which contributes to the refined governance of land use and the enhancement of regional ecological security. Consequently, integrating the attributes of functional zoning and spatial planning objectives is critical for forecasting shifts in land use and evaluating their effects on the relationships among ESs.

The Beijing–Tianjin–Hebei (BTH) region fulfills two essential functions: it acts as a major economic center around China's capital and constitutes an important ecological buffer zone safeguarding northern China. As the largest and most dynamic economic region in northern China, it faces significant challenges. The area's complex and varied topography, intricate landforms, and uneven distribution of socioeconomic resources have led to an increasingly severe imbalance between land supply and demand. This imbalance has intensified the conflict between ecological conservation and development needs. Accelerated urbanization and population concentration over recent decades have triggered widespread encroachment on natural habitats, landscape fragmentation, and environmental pollution. These anthropogenic pressures have caused significant ecosystem degradation, manifested as soil degradation, water resource depletion, and reduced biodiversity [41]. Consequently, the decline in ESs has continued to intensify [42,43]. As a major national development strategy [44], the coordinated development of the Beijing–Tianjin–Hebei region urgently requires systematic ecological planning. This study conducts a systematic assessment of ESs in the BTH region under multiple future development scenarios, focusing on key functional zones. The assessment framework integrates (a) regional natural resource endowments, (b) socioeconomic development demands, and (c) national land-use planning policies. Through this approach, we quantitatively analyze spatiotemporal patterns of ESs trade-offs and synergies, aiming to (i) elucidate the distinction in ESs interactions between functional zones and (ii) establish an evidence-based framework for regional ecosystem management and territorial spatial optimization. Specifically, our research objectives are to (1) develop spatially explicit land-use projections aligned with functional zoning development trajectories; (2) quantify scenario-dependent ESs dynamics and their interrelationships; and (3) characterize zone-specific ESs trade-offs/synergies patterns to inform precision land-use planning. These results provide both theoretical foundations and practical guidelines for achieving ecological security and sustainable development goals in the BTH region.

## 2. Materials and Methods

### 2.1. Study Area and Data Sources

The BTH region is located in the northern part of the North China Plain (36°03′~113°27′ E, 113°27′~119°50′ E), encompassing the municipalities of Beijing and Tianjin, as well as Hebei Province, with a total land area of 216,000 $km^2$. The topography of the study area slopes gradually from northwest to southeast, featuring complex and diverse landforms. The region encompasses multiple terrain types, including plains, hills, basins, mountains,

and plateaus. The study region is characterized by a temperate deciduous broad-leaved forest biome, with natural secondary forests (e.g., *Pinus tabulaeformis Carr*.) dominating mountainous areas. Representative soil types comprise *phaeozems*, *luvisols*, and *solonchaks*. This climatic zone exhibits distinct seasonal contrasts: cold, dry winters versus hot, rainy summers, with an annual average temperature of 11 °C and an annual average precipitation of 500 mm. Hydrologically, the area belongs to the Haihe River basin system, where principal watercourses (e.g., Yongding River and Luan River) predominantly exhibit seasonal flow regimes.

Guided by national land management strategies, local environmental assets—such as variations in elevation—and the spatial structure outlined in the coordinated development of the Beijing–Tianjin–Hebei (BTH) region [18,42], and the zoning of primary functional areas, the BTH area is classified into five distinct units at the county (district) scale. (a) The Bashang Plateau Ecological Protection Zone (BS): As a core area of the ecological security barrier in northern BTH and a functional zone for water conservation serving the capital, this region undertakes critical ecological functions including windbreak and sand fixation, water conservation, and biodiversity maintenance. For future development, it is essential to extensively advance initiatives such as grassland ecological restoration and desertification control, restrict the development of high water-consumption industries, and promote the sustainable development of distinctive agriculture and animal husbandry in a well-regulated manner. (b) The Northwestern Ecological Conservation Zone (ST): This functional area serves as an ecological security barrier and a crucial zone for water conservation and soil preservation in the capital. Together with BS, it forms a multi-tiered and multifunctional ecological circle for the capital. In future development, the strictest ecological protection measures must be implemented, alongside intensified efforts to control soil erosion, so as to safeguard the core functions of the capital. (c) The Central Core Functional Zone (HX): This functional area serves as the core area of the capital's functions and the central zone of the BTH world-class urban agglomeration. It undertakes critical national functions, including central administration, international exchanges, technological innovation, and financial services. In its future development, it is imperative to methodically relocate functions non-essential to the capital, optimize its spatial structure and functional layout, and ultimately establish a polycentric and networked spatial pattern. (d) The Southern Functional Expansion Zone (TZ): This functional area serves as a crucial zone for accommodating industrial relocation from Beijing and Tianjin, as well as an important base for agricultural product production and supply in the BTH region. It undertakes industrial functions such as the commercialization of scientific and technological achievements, advanced manufacturing, and commercial logistics from Beijing and Tianjin, while also playing a vital role in ensuring regional food security. In its future development, the region must actively and systematically absorb industrial transfers, foster the growth of regional central cities, and coordinate efforts to safeguard regional food security. (e) The Eastern Coastal Development Zone (BH): Serving as the coastal gateway to the BTH world-class urban agglomeration, this functional area possesses a cluster of world-class ports, including those in Tianjin, Tangshan, and Huanghua. It functions as a key agglomeration zone for heavy and chemical industries, advanced manufacturing, and the marine economy within the region, while also operating as a demonstration area for marine economic development and ecological conservation. Future development must prioritize steering industries toward high-end and green transformation, alongside strengthening the protection and restoration of coastal ecosystems to enhance regional resilience (Figure 1).

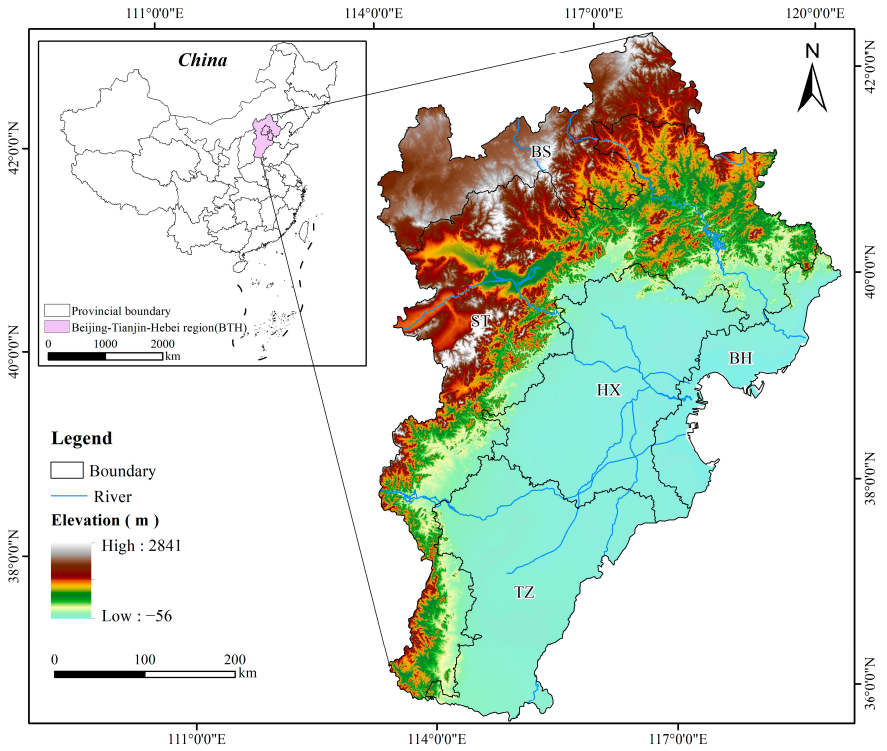



**Figure 1.** Geographical location of the Beijing–Tianjin–Hebei region (BTH).

This research employs land-use information from the years 2000, 2010, and 2020 for the BTH area, supplemented by both natural environmental and socioeconomic data (refer to Table 1). The land cover information was sourced from a nationwide 30 m resolution dataset developed by Professor Yang Jie and Professor Huang Xin's team at Wuhan University. To meet the objectives of the study, the land cover categories were reclassified into six groups: cropland, forest, grassland, water, urbanland, and bareland. Considering the PLUS model's accuracy, regional characteristics, data availability, relevance, and timeliness, we selected elevation, mean annual precipitation, population density, GDP, and other key natural and socioeconomic factors as land-use change drivers. All raster data have a consistent spatial resolution (30 × 30 m), use the Albers Conic Equal Area coordinate system, and share the same extent.

In this study, multiple sources of data were integrated, and the PLUS model along with the InVEST model were employed to predict four typical ESs—habitat quality, carbon storage, water yield, and soil conservation—in BTH region under different scenarios for 2035. Based on the assessment results of ESs, the spatial overlay analysis method is utilized to explore the spatial pattern distribution characteristics of ESs and their trade-offs and synergistic relationships across various functional zones in the region. The specific technical workflow is illustrated in Figure 2.

### *2.2. Land-Use Simulation*

#### 2.2.1. PLUS Model Parameter Settings

In this research, the Markov-PLUS integrated modeling framework is employed to simulate the spatial pattern of land use under three prospective development scenarios within the BTH by 2035. The PLUS model facilitates the simulation of land-use change through a patch-based generative mechanism, integrating the Land Expansion Analysis Strategy (LEAS) with a Cellular Automata (CA) framework powered by a multi-category stochastic seeding system (CARS). The LEAS module requires two temporal snapshots of land-use data and applies random forest algorithms to quantify driving factor impacts on

land expansion. The CARS module simulates land-use competition at local scales, incorporating neighborhood weights and cost matrices derived from LEAS outputs. Neighborhood weights are determined by expansion-to-total area ratios per land type, with adjustments reflecting historical transition trends and functional zone development plans (Table 2). Considering BTH's regional attributes and prior research [45,46], we identified 10 simulation drivers: DEM, slope, precipitation, temperature, soil type, proximity to transport networks/rivers, GDP, and population density.

**Table 1.** Data and descriptions.

| Type | Name | Resolution | Sources |
|---|---|---|---|
| Land use | Land-use types | 30 m | The 30 m land cover dataset for China developed by Professor Yang Jie and Professor Huang Xin's team at Wuhan University |
| Natural factors | Soil types, soil texture, and soil organic matter content | 1 km | Harmonized World Soil Database (HWSD) (http://data.tpdc.ac.cn/zh-hans/, accessed on 3 September 2024) |
| | Precipitation, temperature, and evapotranspiration | 1 km | National Qinghai–Tibet Plateau Data Center (https://data.tpdc.ac.cn/, accessed on 3 September 2024) |
| | DEM, and slope | 30 m | Geospatial Data Cloud (https://www.gscloud.cn/, accessed on 3 September 2024) |
| Socioeconomic | Population density and GDP | 1 km | Resource and Environment Data Cloud Platform (https://www.resdc.cn/DOI/, accessed on 3 September 2024) |
| | Distance from rivers, railways, and highways | 500 m | National Catalogue Services For Geographic Information (https://www.webmap.cn/, accessed on 3 September 2024) |
| Administrative boundaries | Administrative boundary vector map of the BTH | -- | National Geomatics Center of China (https://www.ngcc.cn/, accessed on 3 September 2024) |

**Table 2.** Neighborhood weights.

| Land-Use Type | BS | | | ST | | | HX | | | TZ | | | BH | | |
|---|---|---|---|---|---|---|---|---|---|---|---|---|---|---|---|
| | ND | EP | EC | ND | EP | EC | ND | EP | EC | ND | EP | EC | ND | EP | EC |
| Cropland | 0.35 | 0.42 | 0.32 | 0.35 | 0.38 | 0.31 | 0.35 | 0.36 | 0.29 | 0.35 | 0.4 | 0.34 | 0.35 | 0.36 | 0.28 |
| Forest | 0.15 | 0.3 | 0.12 | 0.15 | 0.31 | 0.13 | 0.15 | 0.18 | 0.11 | 0.15 | 0.25 | 0.11 | 0.15 | 0.2 | 0.1 |
| Grassland | 0.08 | 0.13 | 0.09 | 0.08 | 0.15 | 0.07 | 0.08 | 0.09 | 0.06 | 0.08 | 0.1 | 0.05 | 0.08 | 0.09 | 0.06 |
| Water | 0.09 | 0.12 | 0.07 | 0.09 | 0.11 | 0.09 | 0.09 | 0.08 | 0.08 | 0.09 | 0.1 | 0.07 | 0.09 | 0.1 | 0.08 |
| Urbanland | 0.7 | 0.64 | 0.8 | 0.7 | 0.6 | 0.74 | 0.7 | 0.61 | 0.76 | 0.7 | 0.7 | 0.89 | 0.7 | 0.68 | 0.9 |
| Bareland | 0.01 | 0.01 | 0.01 | 0.01 | 0.01 | 0.01 | 0.01 | 0.01 | 0.01 | 0.01 | 0.01 | 0.01 | 0.01 | 0.01 | 0.01 |

Employing land cover data from 2010 as a reference, we projected the spatial pattern of land use for the year 2020 and conducted subsequent accuracy assessments. The evaluation outcomes revealed a strong concordance, with a Kappa coefficient of 0.86, and an overall classification accuracy of 90%. These metrics confirm the robustness and applicability of the modeling framework for forecasting land-use changes within the BTH area.

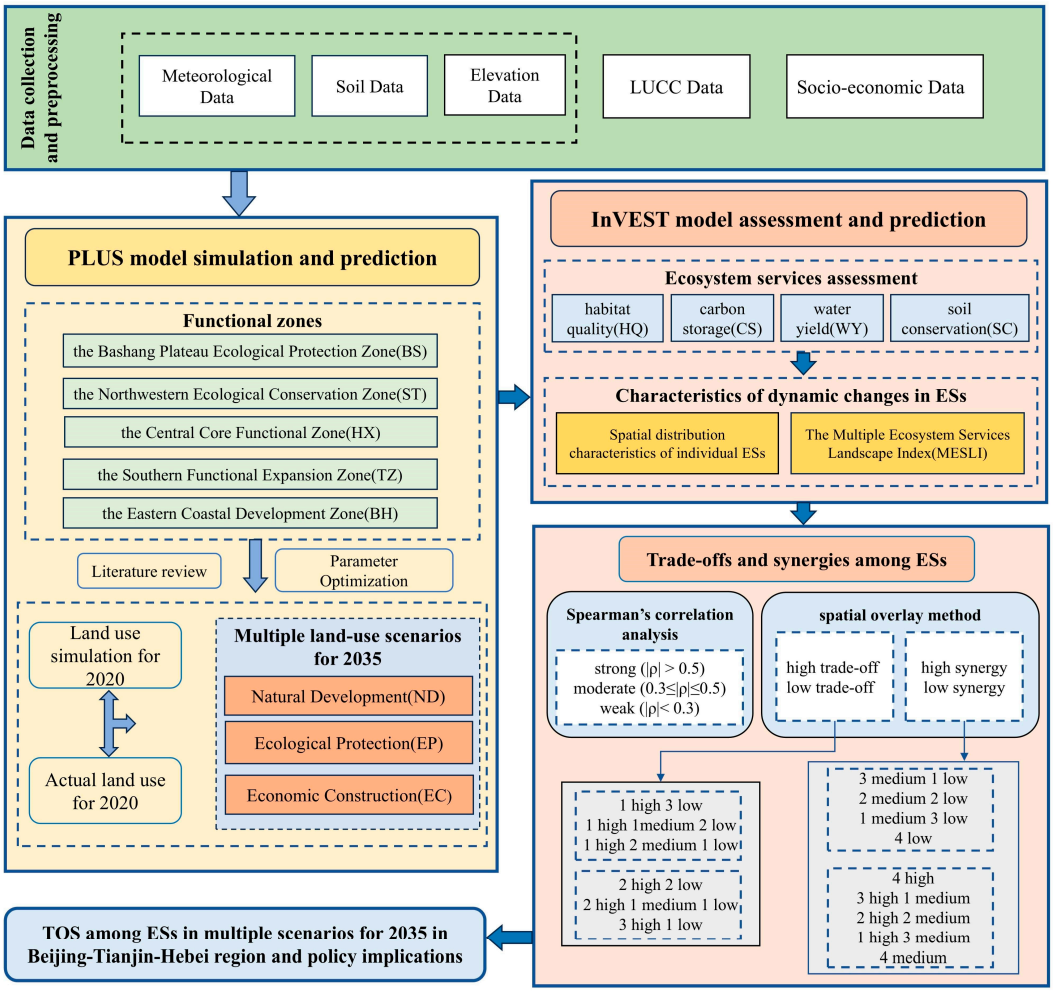



**Figure 2.** Technical flow chart of this study.

### 2.2.2. Scenario Setting

Taking into account the Coordinated Development of the Beijing–Tianjin–Hebei Region, the Beijing Territorial Space Master Plan (2021–2035), the Tianjin Territorial Master Plan (2021–2035), the Hebei Territorial Space Planning (2021–2035), and the Hebei Major Function-Oriented Zone Planning and considering the future development needs of each functional zone as well as regional land-use policy preferences, this research examined the directions of land-use conversions between 2000 and 2020 in order to calibrate the transition probability and cost matrix. We established three scenarios: Natural Development (ND), Ecological Protection (EP), and Economic Construction (EC). Scenario configurations were established in the following manner: ND scenario, simulating baseline trends while excluding policy interventions, with water bodies designated as protected areas based on 2000–2020 transition patterns to project 2035 land-use distributions; EP scenario, prioritizing ecological conservation, with this scenario incorporating functional zone-specific transition probabilities with nature reserves and water bodies as no-conversion zones; and EC scenario, emphasizing economic growth and featuring reduced conversion probabilities from built-up areas and enhanced transitions to urbanland, while maintaining nature reserves and water bodies as protected zones. The cost matrices and transition probability adjustment schemes for each functional zone under different scenarios can be found in the Supplementary Materials.

### 2.3. Assessment of Ecosystem Services

Given the study area's natural resource endowment, socioeconomic characteristics, and regional development needs, four key ESs served as indicators in the research: habitat quality (HQ), carbon storage (CS), water yield (WY), and soil conservation (SC). In this study, the InVEST model was used to quantitatively evaluate the spatiotemporal pattern of four key ESs. Table 3 presents the model parameters and computational procedures. All raster data involved in the formula were resampled to a resolution of 30 × 30 m to match the resolution of the LUCC data.

**Table 3.** Metrics and approaches applied to the quantification of diverse ESs.

| Services Type | Methodology | Calculation Formula | Meaning of Indicators |
| --- | --- | --- | --- |
| HQ | The HQ module in the InVEST model is calculated based on an analysis of LUCC and its associated threats to biodiversity [47]. For the key parameters, see the Supplementary Materials. | $Q_{xj} = H_j\left(1 - \frac{D_{xj}^Z}{D_{xj}^Z + K^Z}\right)$ | $H_j$ is the habitat suitability scores of land-use type $j$; $z$ represents a normalization constant, generally taken to be 2.5; $D_{xj}$ is the habitat degradation index of grid $x$ in land-use type $j$; K represents the half-saturation constant, typically taken as half the maximum value of $D_{xj}$; and $Q_{xj}$ represents the habitat quality index of grid $x$ in land-use type $j$ |
| CS | The carbon storage and sequestration module of the InVEST model is used to estimate CS [26]. For the key parameters, see the Supplementary Materials. | $C_{total} = C_{above} + C_{below} + C_{soil} + C_{dead}$<br>$C_{totali} = (C_{abovei} + C_{belowi} + C_{soili} + C_{deadi}) \times A_i$ | $C_{totali}$ is the average carbon density of land-use category $i$, and Ai represents the corresponding area; $C_{total}$ is the total carbon storage in the Beijing–Tianjin–Hebei region (t/hm$^2$); and $C_{above}$, $C_{below}$, $C_{soil}$, and $C_{dead}$ represent above-ground carbon storage, below-ground carbon storage, soil carbon storage, and the dead carbon storage capacity, in t/hm$^2$, respectively |
| WY | The InVEST model's water balance principle is used to estimate the WY. This module determines the WY of each grid based on the water-balancing principle by deducting the actual evapotranspiration from the rainfall [47]. For the key parameters, see the Supplementary Materials. | $Y_{xj} = \left(1 - \frac{AET_{xj}}{P_x}\right) \times P_x$ | $AET_{xj}$ represents the annual actual evapotranspiration of grid $x$ in land-use category $j$; $P_x$ represents the annual precipitation of grid $x$; and $Y_{xj}$ represents the water yield of grid $x$ in land-use type $j$ |
| SC | The Sediment Delivery Ratio module of the InVEST model is used to estimate SC [47]. For the key parameters, see the Supplementary Materials. | $RKLS = R \times K \times LS\ ULSE = R \times K \times LS \times P \times C\ SC = RKLS - ULSE$ | $SC$ represents the annual soil conservation quantity; $C$ corresponds to the vegetation cover and management factor, while $P$ indicates the support practice factor for soil conservation; $K$ stands for the soil erodibility factor; $R$ denotes the rainfall erosivity index, derived from yearly precipitation data; and the topographic factor, $LS$, is computed using slope gradient and slope length |

### 2.4. Calculation of the Multiple Ecosystem Service Landscape Index

The Multiple Ecosystem Service Landscape Index (MESLI) was employed to evaluate the comprehensive ecosystem capacity of the study region. As a robust and comprehensive environmental metric, MESLI captures the capacity of diverse ecosystems to deliver multiple ESs concurrently [48,49]. The index is computed by aggregating standardized indicators of individual ESs [50], facilitating the identification of spatial patterns such as cold spots and hot spots across service bundles. Prior to aggregation, each ecosystem

service variable is standardized to mitigate discrepancies in measurement units. The raster data in the formula have a resolution of 30 × 30 m.

$$MESLI = \sum_{i=1}^{n} \frac{x_i - min(x_i)}{max(x_i) - min(x_i)} \quad (1)$$

In this formula, the variable $i$ denotes a specific category of ESs, while n suggests the total count of such service types considered. The term $x_i$ corresponds to the measured value for the $i_{\text{th}}$ service category. Additionally, max($x_i$) and min($x_i$) refer to the highest and lowest observed values, respectively, for that particular category of ecosystem service.

### *2.5. Methods for Quantifying Trade-Offs and Synergies Among Ecosystem Services*

Given the distributional features of ESs data, Spearman's correlation analysis was employed to assess trade-offs and synergies between ESs both across the entire study area and within individual functional zones in the BTH region. The analysis was conducted for the baseline year 2020 and under three different scenarios projected for 2035. In the resulting correlation matrices, blue denotes a positive relationship, while red signifies a negative association. Deeper color shades and larger circle sizes correspond to stronger correlation magnitudes. The strength of correlation was classified into three tiers: strong ($|\rho| > 0.5$), moderate ($0.3 \leq |\rho| \leq 0.5$), and weak ($|\rho| < 0.3$). The computational formula applied in this analysis is provided below:

$$\rho = \frac{\frac{1}{n}\sum_{i=1}^{n}\left(R(x_i) - \overline{R(x)}\right) \times \left(R(y_i) - \overline{R(y)}\right)}{\sqrt{\left(\frac{1}{n}\sum_{i=1}^{n}\left(R(x_i) - \overline{R(x)}\right)^2\right) \times \left(\frac{1}{n}\sum_{i=1}^{n}\left(R(y_i) - \overline{R(x)}\right)^2\right)}} \quad (2)$$

In this formula, $R(x_i)$ and $R(y_i)$ refer to the rank values of $x_i$ and $y_i$, while $R(x)$ and $R(y)$ refer to the mean ranks of the variables $x$ and $y$, respectively. The symbol ρ represents the correlation coefficient between variables $x$ and $y$, which ranges from −1 to 1. A larger absolute value of $|\rho|$ signifies a stronger correlation between the variables. A positive value of ρ suggests a synergistic relationship (positive correlation), whereas a negative value suggests a trade-off (negative correlation) between the variables.

### *2.6. Spatial Assessment of Trade-Offs and Synergies Among Ecosystem Services*

The spatial overlay method provides a ranking-based framework for quantifying trade-offs and synergistic interactions among ESs. The approach classifies ESs supply capacities, performs spatial overlays, and evaluates inter-service relationships based on relative quantity levels. The trade-off effect describes a situation within a spatial unit where one or two services have strong supply capacities while others are weak. The synergy effect refers to a state where multiple services all have either strong or weak supply capacities [51]. This study employed ArcGIS 10.8 software to categorize standardized ecosystem service values into low, medium, and high tiers using the natural breakpoint method, assigning them codes 1, 2, and 3, respectively. Based on these results, raster data underwent spatial overlay analysis according to the following rules [26,52], classifying them into two categories: high/low trade-off and high/low synergy. Table 4 details the classification criteria.

$$CODE = A \times 1000 + B \times 100 + C \times 10 + D \times 1 \quad (3)$$

**Table 4.** Methods for classifying relationships among ESs.

| Service Relationship | Type | Supply Capacity Mix | Number of Combinations |
|---|---|---|---|
| trade-off | high trade-off | 1 high 3 low | 4 |
| | | 1 high 1 medium 2 low | 12 |
| | | 1 high 2 medium 1 low | 12 |
| | low trade-off | 2 high 2 low | 6 |
| | | 2 high 1 medium 1 low | 12 |
| | | 3 high 1 low | 4 |
| synergy | low synergy | 3 medium 1 low | 4 |
| | | 2 medium 2 low | 6 |
| | | 1 medium 3 low | 4 |
| | | 4 low | 1 |
| | high synergy | 4 high | 1 |
| | | 3 high 1 medium | 4 |
| | | 2 high 2 medium | 6 |
| | | 1 high 3 medium | 4 |
| | | 4 medium | 1 |

In the formula, CODE is the four-digit overlay code, and A, B, C, and D are HQ, CS, WY, and SC, respectively.

## 3. Results

### *3.1. Analysis of LUCC Characteristics*

The BTH region is primarily composed of cropland (43.80%) and forest (24.98%), which together account for 68.78% of the total land area in 2020. Projections of land-use changes from 2020 to 2035 indicate significant shifts between cropland, forest, and urbanland, with their proportional distributions varying depending on the scenario: (1) Cropland area exhibits a general decreasing trend; however, this decline is substantially alleviated under the EP scenario. Under EP, cropland is projected to maintain the highest proportion (41.01%) among all land-use types by 2035. (2) Forest area demonstrates a consistent upward trend, with the most notable expansion observed under the EP scenario, reaching an increase of $3.78 \times 10^3$ km$^2$—representing a growth of 26.73%. (3) Urbanland shows a gradual growth trend driven by urbanization, with the highest proportion in the EC scenario (19.18% in 2035, compared to 15.04% in 2020). In contrast, the ND scenario reflects a slower pace of land-use transformation. Other land categories (grassland, water, and bareland) remain stable across all scenarios (Figure 3). Notably, by 2035, spatial distribution differences in land-use types are minimal across different scenarios.

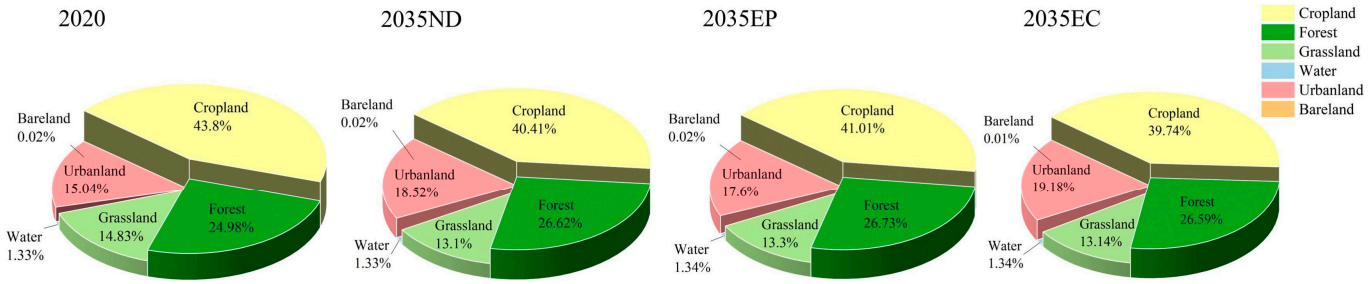



**Figure 3.** Area proportion of each land-use type in BTH.

Regarding the spatial allocation of various land-use categories, cropland is predominantly located in HX and TZ, comprising 65.43% and 74.70% of each zone's total area, respectively. Owing to substantial spatial overlap with regions suitable for urban expansion,

approximately 7% of the cropland within these zones was transformed into urbanland under the ND scenario. Under the EP scenario, however, the conversion of cropland was strategically limited to support regional agricultural sustainability, leading to the highest retention of cropland area among all scenarios. Forest and grassland are concentrated predominantly in BS and ST, and together they constitute more than half of the land cover across all functional zones in each of the three scenarios. With ecological preservation as a central goal under the EP scenario, the transfer of ecologically valuable land was regulated, contributing to a net increase in forest area of 1626.63 $km^2$ (5.16%) and 2105.92 $km^2$ (2.27%) in the two principal functional regions. Water within the BTH region are largely situated in BH, and their extent remains relatively stable under all projected scenarios. Urbanland occupies a significant share of HX and TZ, representing one of the two predominant types of land used there. In contrast, bareland covers a minimal portion (0.02%) of the entire study area (Figure 4).

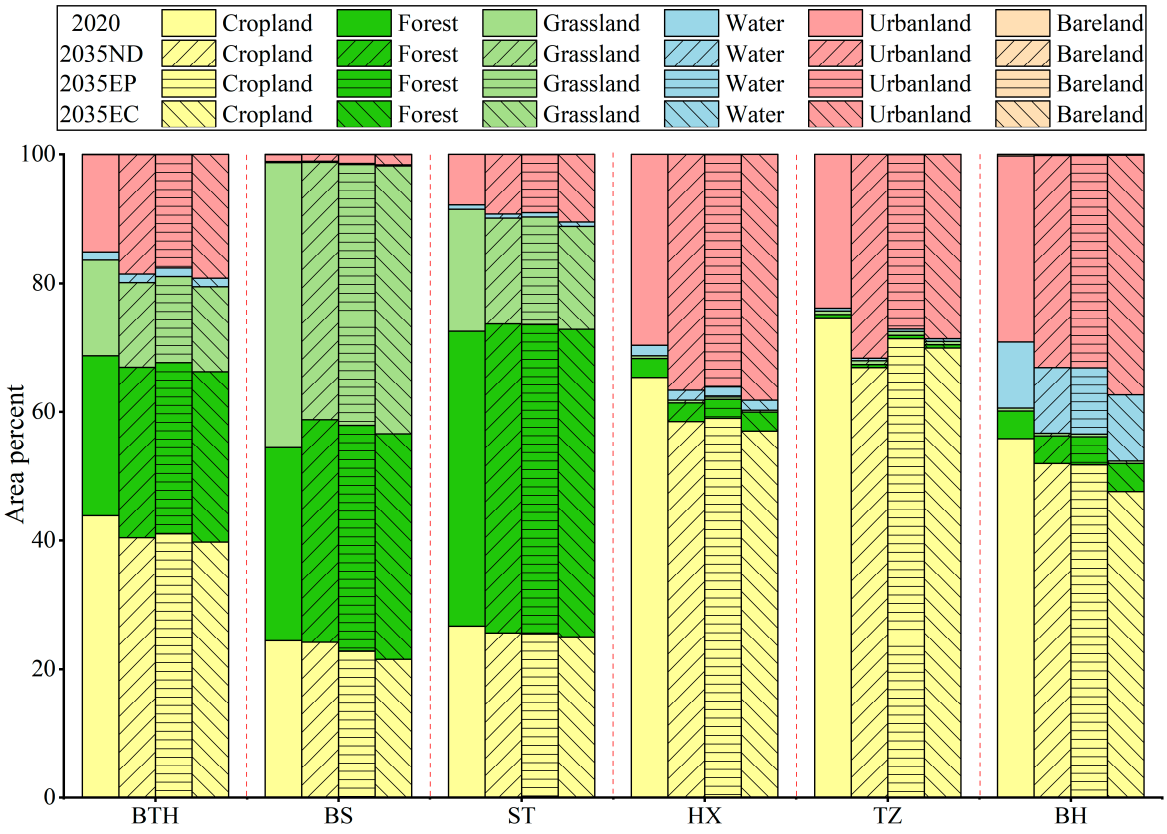



**Figure 4.** Proportion of land-use types in BTH and different functional zones.

### *3.2. Characteristics of Dynamic Changes in ESs*

#### 3.2.1. Spatial Distribution Characteristics of Individual ESs

The spatial heterogeneity of the four ESs within the BTH region is illustrated in Figure 5. HQ and CS display comparable spatial configurations, characterized by elevated values predominantly in regions with extensive ecological land cover—such as BS and ST—and lower values largely found in areas with high densities of constructed surfaces, including HX, TZ, and BH. SC exhibits a spatial pattern strongly associated with the topographic gradient, displaying higher values in the northwestern mountainous regions and diminished values across the southeastern plains. In contrast, WY demonstrates a spatial distribution inverse to the other three services, with elevated levels observed in the southeastern parts of the region—notably in BH—and reduced levels in the northwestern zones, specifically BS and ST.

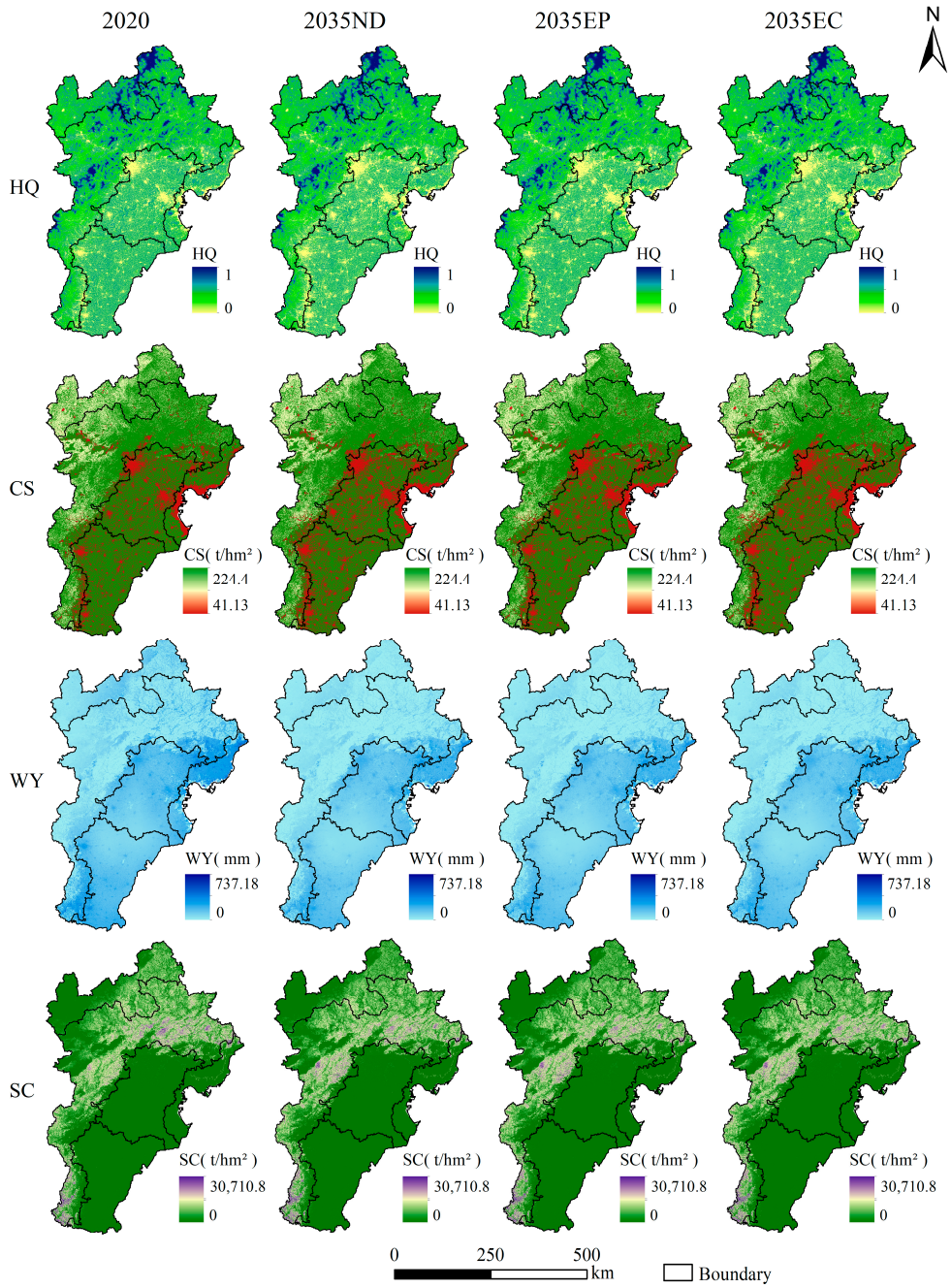



**Figure 5.** Spatial patterns of individual ESs across the BTH region.

Compared with 2020, the four ESs showed varying degrees of change in the three scenarios (Table 5). Specifically, compared with 2020, HQ showed a downward trend in all three scenarios by 2035, with the mean values ranked from highest to lowest as EP (0.2590) > ND (0.2564) > EC (0.2543). In different scenarios, the total amount of CS increased in both the ND and EP scenarios, from 25.49 $\times$ $10^8$ t to 25.58 $\times$ $10^8$ t and 25.71 $\times$ $10^8$ t, respectively, while it decreased by 0.01 $\times$ $10^8$ t in the EC scenario. The three scenarios are ranked from largest to smallest as EP > ND > EC. WY decreased to some extent in all three scenarios, with the largest decrease occurring in the EP scenario, amounting to 164.55 $\times$ $10^8$ $m^3$. The total volume ranked as EC > ND > EP across the three scenarios. Compared with 2020, SC also decreases to a certain extent in future scenarios. From different scenarios, SC shows the smallest decrease in the ND scenario, which is 55.31 $\times$ $10^8$ t. In the three scenarios, the total amount of SC is ranked from large to small as ND > EC > EP.

**Table 5.** Changes in individual ESs across the BTH region.

| | HQ | Change/% | CS /($10^8$ t) | Change/% | WY /($10^8$ $m^3$) | Change/% | SC /($10^8$ t) | Change/% |
|---|---|---|---|---|---|---|---|---|
| 2020 | 0.2659 | --- | 25.49 | --- | 230.21 | --- | 264.11 | --- |
| 2035ND | 0.2564 | −3.57 | 25.58 | 0.35 | 165.62 | −28.06 | 208.80 | −20.94 |
| 2035EP | 0.2590 | −2.59 | 25.71 | 0.86 | 164.55 | −28.09 | 208.51 | −21.05 |
| 2035EC | 0.2543 | −4.36 | 25.48 | −0.04 | 166.82 | −27.54 | 208.64 | −21.00 |

#### 3.2.2. Spatial Distribution Characteristics of Multiple Ecosystem Service Provisioning Capacities

Figure 5 reveals the spatial pattern of the MESLI across the BTH region for the baseline year 2020 and under three projected scenarios for 2035. The mean MESLI values for 2020 and the 2035 ND, EP, and EC scenarios are 0.8713, 0.8312, 0.8365, and 0.8274, respectively. These results indicate an overall decline in the ability of the BTH region to provide multiple ecosystem services by 2035 compared to the 2020 baseline. However, there are slight differences in the average MESLI values across different scenarios, with the order from highest to lowest being EP > ND > EC. This suggests that under the EP scenario in 2035, the BTH region has a stronger capacity to provide various ESs (Figure 6a). There are significant differences in the average MESLI values among the five functional zones in the BTH region. BS and ST have higher average MESLI values, indicating that these two functional zones have a higher comprehensive capacity to provide multiple ecosystem services, while HX and TZ have lower average MESLI values, indicating that these functional zones have a lower level of supply capacity for multiple ecosystem services. Overall, the average MESLI values across the three scenarios for 2035 show little difference among the functional zones (Figure 6b–f).

Employing the natural breaks classification method, MESLI values were categorized into three tiers: low (0–0.5), moderate (0.5–1.2), and high (>1.2). The results reveal pronounced spatial heterogeneity in MESLI across the BTH region, characterized by a northwest-high and southeast-low spatial gradient (Figure 7). Areas with high MESLI values are predominantly distributed in zones of substantial vegetation cover, such as BS and ST, whereas moderate values are primarily observed in the southeastern functional zones of HX, TZ, and BH. These three functional zones are located in plains with flat terrain and are easily affected by human activities, resulting in a relatively limited range of ESs they can provide. Low values are predominantly concentrated in urbanized areas across the functional zones, particularly within the central sectors of HX and BH, where the provision of ESs remains comparatively limited. A comparison of the areas of each level in the three scenarios for 2035 shows that in the EP scenario, the area of high-value zones accounts for the largest proportion compared to other scenarios, while the area of low-value zones accounts for the smallest proportion. Conversely, in the EC scenario, the area of high-value zones accounts for the smallest proportion, while the area of low-value zones accounts for the largest proportion (Table 6).

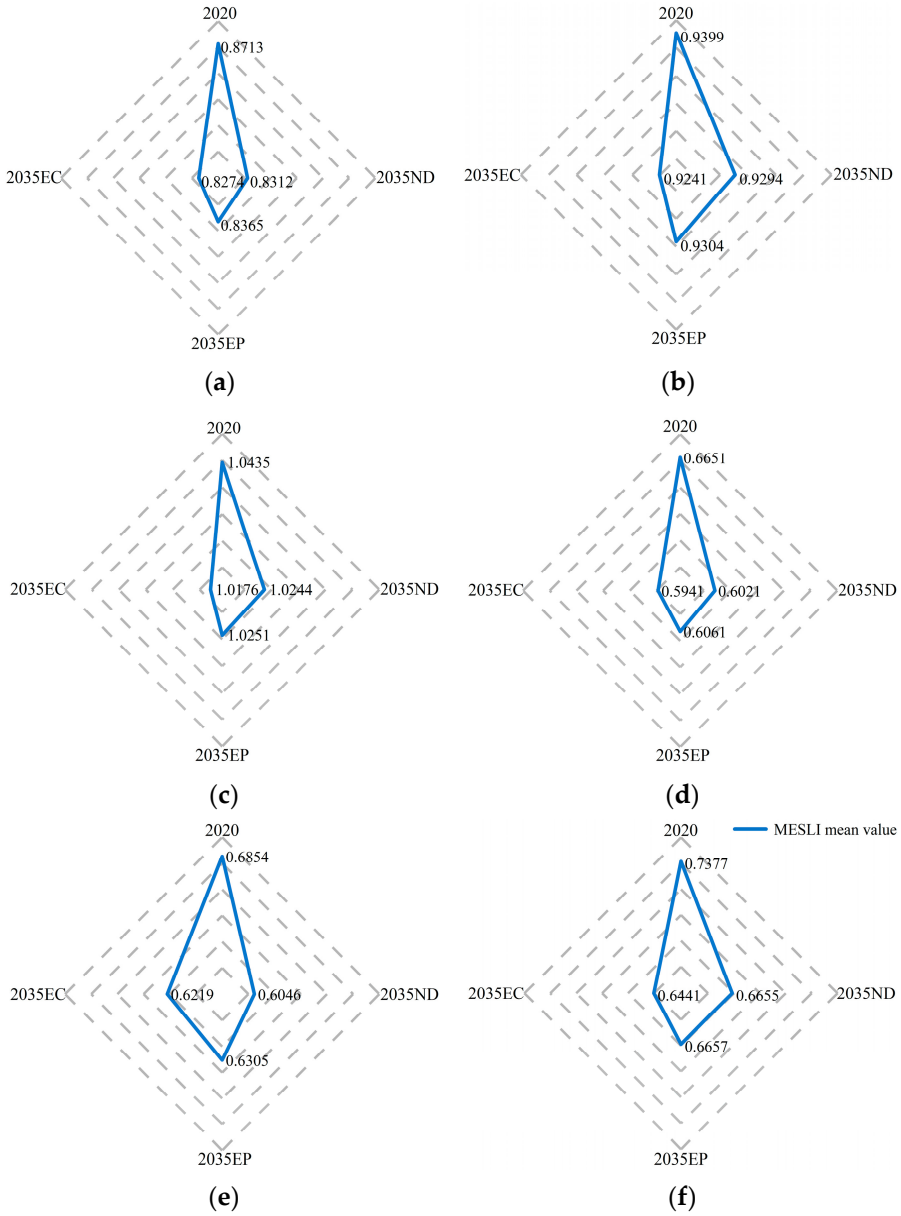



**Figure 6.** Average MESLI values for the BTH region and functional zones under different scenarios from 2020 to 2035: (**a**) average MESLI values for the BTH region; (**b**) average MESLI values for BS; (**c**) average MESLI values for ST; (**d**) average MESLI values for HX; (**e**) average MESLI values for TZ; (**f**) average MESLI values for BH.

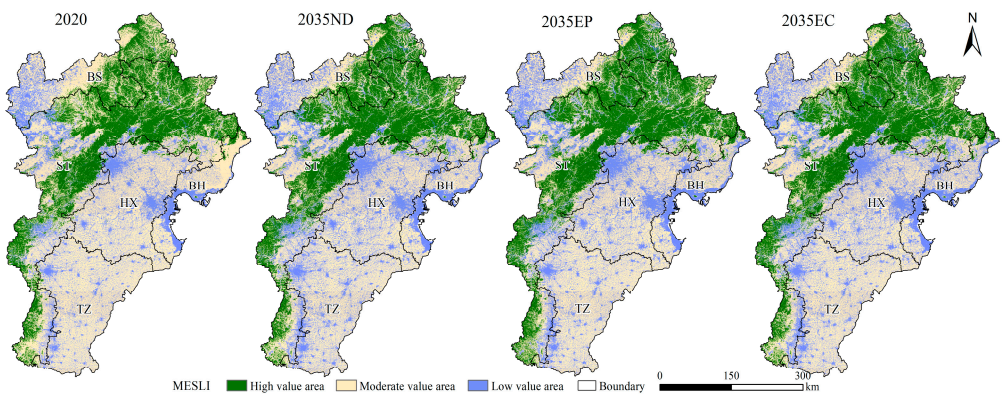



**Figure 7.** Spatial distribution of MESLI for the BTH region under different scenarios from 2020 to 2035.

**Table 6.** Area and proportion of each MESLI level in BTH.

| [1] | Low-Value Area | Moderate-Value Area | High-Value Area |
|---|---|---|---|
| 2020 | 43.46 (20.14) | 118.31 (54.83) | 54.03 (25.04) |
| 2035ND | 55.41 (25.67) | 102.96 (47.71) | 57.43 (26.61) |
| 2035EP | 53.49 (24.79) | 104.65 (48.50) | 57.65 (26.71) |
| 2035EC | 56.28 (26.08) | 102.17 (47.35) | 57.34 (26.57) |

[1] The values outside the parentheses indicate the area, with the unit being $10^3$ km$^2$. The values inside the parentheses indicate the percentage, with the unit being %.

### *3.3. Characteristics of Changes in Trade-Offs and Synergies of ESs*

#### 3.3.1. Correlation Characteristics Between ESs

This research applied Spearman's correlation analysis to assess trade-offs and synergies among ESs in 2020 and 2035 for three development scenarios (EP, EC, and ND) in both the entire BTH region and its functional zones (Figure 8). The analysis revealed that all four ESs showed statistically significant correlations at the regional level ($p < 0.001$). In 2020, HQ_CS displayed the strongest synergy ($\rho = 0.51$), while CS_WY showed the strongest trade-off ($\rho = -0.56$). By 2035, both trade-offs and synergies intensities increased across all scenarios, with varying degrees of enhancement: the HQ_CS and CS_SC synergy strengthened most notably in the ND scenario; the CS_WY trade-off intensified most significantly in the EC scenario ($\rho = -0.62$).

From a functional zoning perspective, the trade-offs and synergies relationships among ESs exhibit pronounced patterns across different zones. In both BS and ST, the four ESs display consistent interaction characteristics. Specifically, HQ, CS, and SC show synergistic effects with one another, whereas WY demonstrates a trade-off relationship with the other three services. Compared to the baseline year 2020, interactions among regional ESs have intensified under all three 2035 scenarios, though the magnitude of trade-offs and synergies remains relatively consistent across these scenarios. Furthermore, the nature of trade-off and synergistic relationships between identical ESs pairs differs between the two functional zones. For example, the synergistic relationship between CS and SC and the trade-off relationship between CS and WY in ST are stronger than those in BS. Additionally, the four ESs demonstrate consistent trade-off and synergy patterns in both HX and TZ. However, the interactions within the six ESs pairs differ in the extent of changes observed across the three 2035 scenarios. Compared to 2020, the synergistic interactions between HQ and CS strengthen across both functional zones under all three 2035 scenarios. Conversely, trade-off effects between HQ and WY as well as between CS and WY intensify in HX, while the trade-off between CS and WY weakens in TZ. For BH, all six pairs of ESs show synergistic relationships, and all are statistically significant ($p < 0.05$). Among them, HQ_CS exhibits a strong synergistic relationship ($|\rho| > 0.5$), CS_SC and SC_WY exhibit a moderate synergistic relationship ($0.3 \leq |\rho| \leq 0.5$), and the rest exhibit a weak synergistic relationship. Compared with 2020, the six pairs of ESs correlations exhibit different patterns of change under the three scenarios in 2035. Except for the enhanced synergistic effect of HQ_CS, the synergistic effects of the remaining five ESs pairs all showed varying degrees of weakening (Table 7).

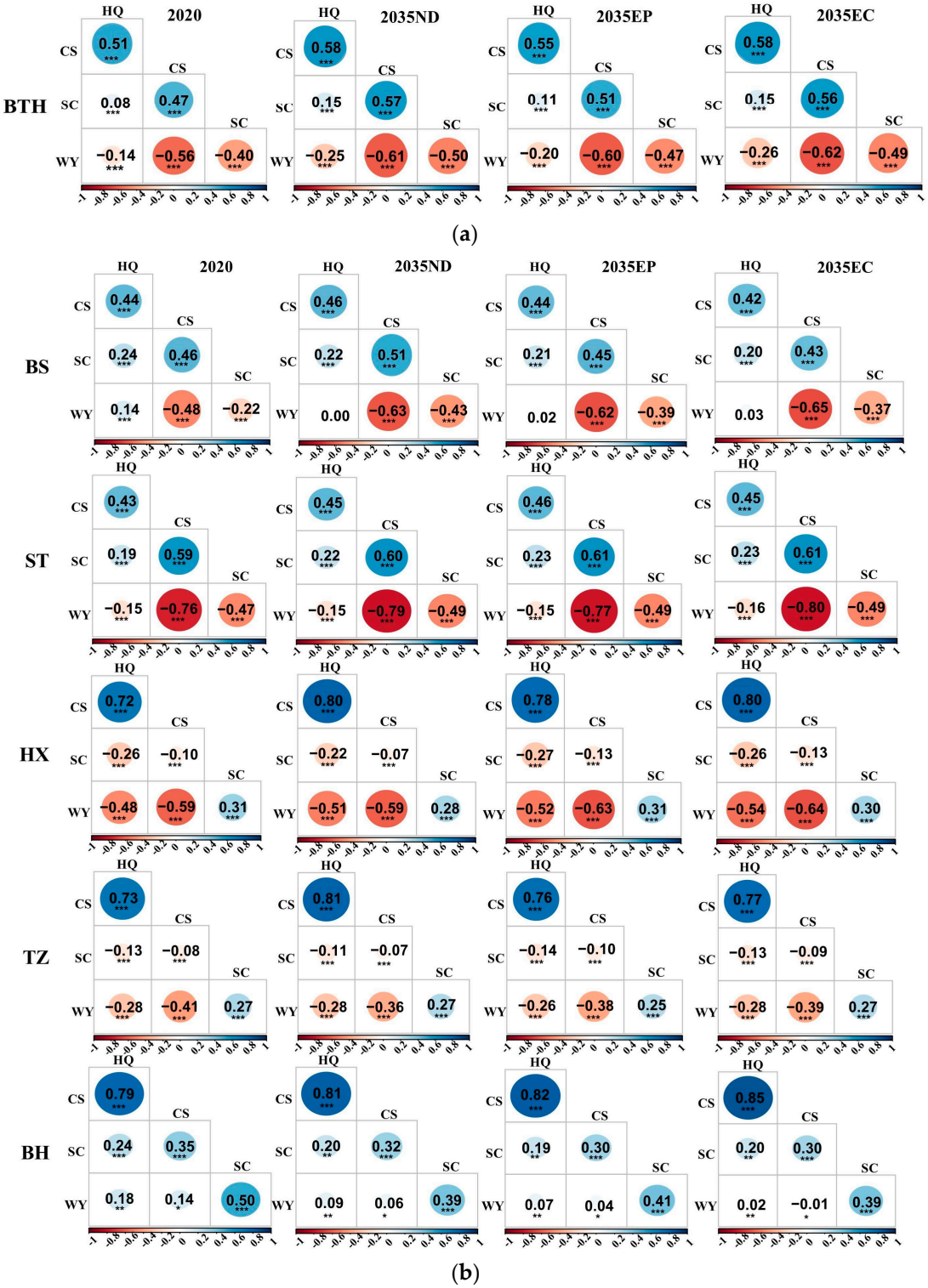



**Figure 8.** Correlation between ESs in the BTH region and functional zones in 2020 and 2035 under three scenarios (* indicates $p < 0.05$, ** indicates $p < 0.01$, and *** indicates $p < 0.001$): (**a**) correlation between ESs in BTH; (**b**) correlation between ESs in various functional zones.

**Table 7.** Change in correlation coefficients between ESs in the BTH region and functional zones from 2020 to 2035 for three scenarios.

| | | HQ_CS | HQ_SC | CS_SC | HQ_WY | CS_WY | SC_WY |
|---|---|---|---|---|---|---|---|
| BTH | 2020–2035ND | +0.07 | +0.07 | +0.10 | −0.11 | −0.05 | −0.10 |
| | 2020–2035EP | +0.04 | +0.03 | +0.04 | −0.06 | −0.04 | −0.07 |
| | 2020–2035EC | +0.07 | +0.07 | +0.09 | −0.12 | −0.06 | −0.09 |
| BS | 2020–2035ND | +0.02 | −0.02 | +0.05 | −0.14 | −0.15 | −0.21 |
| | 2020–2035EP | 0 | −0.03 | −0.01 | −0.12 | −0.14 | −0.17 |
| | 2020–2035EC | −0.02 | −0.04 | −0.03 | −0.11 | −0.17 | −0.15 |
| ST | 2020–2035ND | +0.02 | +0.03 | +0.01 | 0 | −0.03 | −0.02 |
| | 2020–2035EP | +0.03 | +0.04 | +0.02 | 0 | −0.01 | −0.02 |
| | 2020–2035EC | +0.02 | +0.04 | +0.02 | −0.01 | −0.04 | −0.02 |
| HX | 2020–2035ND | +0.08 | +0.04 | +0.03 | −0.03 | 0 | −0.03 |
| | 2020–2035EP | +0.06 | −0.01 | −0.03 | −0.04 | −0.04 | 0 |
| | 2020–2035EC | +0.08 | 0 | −0.03 | −0.06 | −0.05 | −0.01 |
| TZ | 2020–2035ND | +0.08 | +0.02 | +0.01 | 0 | +0.05 | 0 |
| | 2020–2035EP | +0.03 | −0.01 | −0.02 | +0.02 | +0.03 | −0.02 |
| | 2020–2035EC | +0.04 | 0 | −0.01 | 0 | +0.02 | 0 |
| BH | 2020–2035ND | +0.02 | −0.04 | −0.03 | −0.09 | −0.08 | −0.11 |
| | 2020–2035EP | +0.03 | −0.05 | −0.05 | −0.11 | −0.10 | −0.09 |
| | 2020–2035EC | +0.06 | −0.04 | −0.05 | −0.16 | −0.13 | −0.11 |

Overall, the correlation coefficients of ESs in various functional zones differ significantly from the entire region in BTH. Furthermore, the relationships and strengths between ESs vary across different functional zones depending on their types and spatial locations. Similarities and differences exist in the trade-off synergies between similar services across different functional zones.

#### 3.3.2. Distribution Characteristics of Trade-Offs and Synergies Among ESs

The results of the spatial overlay analysis revealed substantial disparities among ESs within the BTH region (Figure 9). Specifically, high-synergy areas are primarily located in BS, as well as the northern and the southern region of ST. Low-synergy areas are mainly distributed in the western regions of BS and ST, as well as the central plain region of the study area. Areas characterized by low trade-offs are predominantly concentrated in the northern part of the study region, specifically within certain northern sections of BS and ST. In contrast, regions with high trade-off values are mainly located in BH, with minor occurrences also found in the southern area of the study region. Furthermore, the distribution characteristics of trade-offs remain relatively consistent across the three scenarios projected for 2035. Notably, however, compared to the baseline conditions in 2020, the proportion of ESs trade-offs between different functional zones will differ in 2035 (Figure 10). The relationships between ESs in the BS region are primarily characterized by low synergistic relationships, accounting for 49% in 2020. Under the three future scenarios, the proportion of low synergistic relationships increases, while the proportion of high synergistic relationships decreases. Nevertheless, in the EP scenario, the proportion of areas exhibiting high synergistic relationships exceeds that observed in the other scenarios. In ST, high trade-offs and low synergies dominate the interactions among ESs. In 2020, these interaction types accounted for 34% and 30% of the regional area, respectively. By 2035, the proportional distribution of different levels of trade-off and synergistic relationships shows minimal variation across the three scenarios; however, the EC scenario has the lowest proportion of high synergistic relationships, accounting for only 9%. Relationships between ESs in HX and TZ are primarily characterized by low synergistic relationships, accounting for 72% and 78%, respectively, and the proportion of this level decreases in

all three scenarios by 2035, while the proportion of high synergistic relationships remains largely unchanged. In the coastal BH region, interactions among ESs are predominantly characterized by high trade-offs, comprising 69% of the area. By 2035, the proportion of high trade-off areas increases, whereas regions with low synergies decrease. Changes in other categories of trade-offs and synergies remain relatively limited; however, under the EP scenario, the share of highly synergistic relationships, though still modest at 3%, exceeds that of the other scenarios.

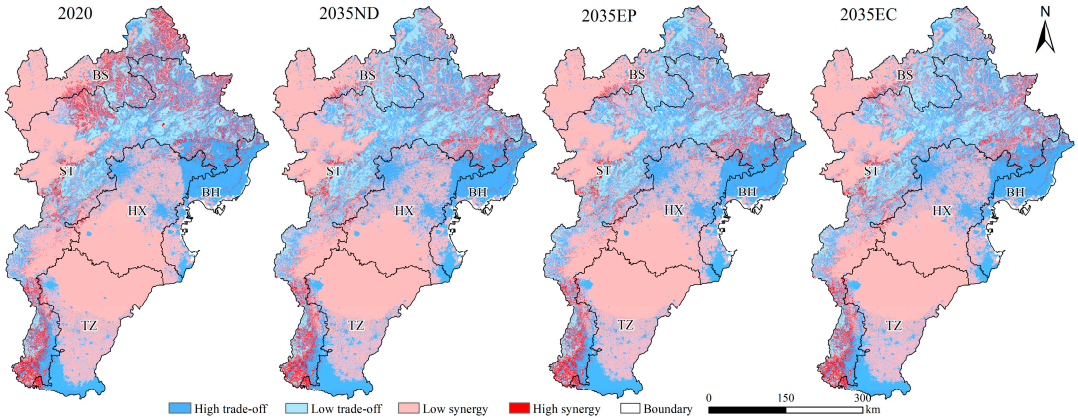



**Figure 9.** Distribution of trade-offs and synergies between ESs in BTH.

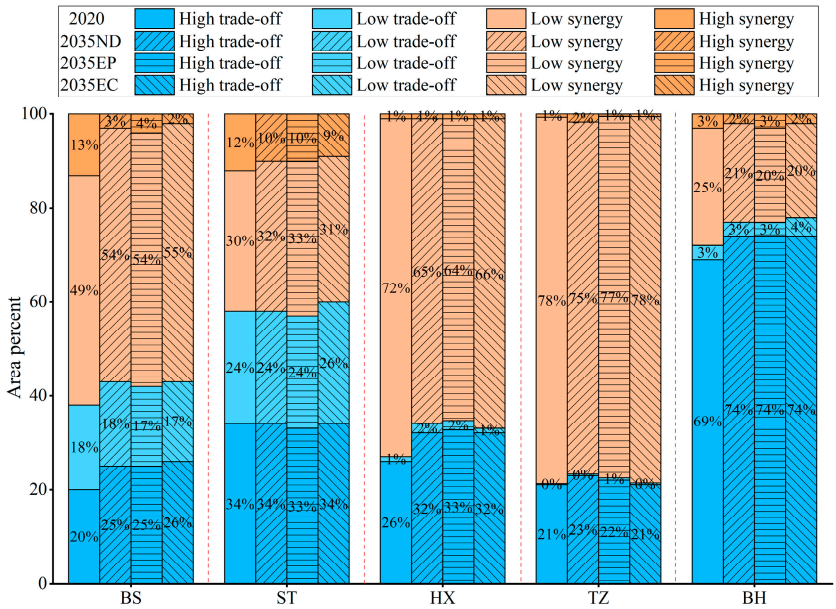



**Figure 10.** Proportion of trade-offs and synergies between ESs in BTH.

## 4. Discussion

### *4.1. Impacts of Land-Use Changes on ESs*

Existing studies indicate that pronounced spatial heterogeneity in ESs is strongly linked to the spatial characteristics of socio-natural drivers [53], particularly land-use factors. In this study, the parameters required for the PLUS and InVEST models were determined based on the relevant literature [43,44,54] and adjusted according to the study region characteristics, thereby ensuring the credibility of the research findings. The results of the research reveal that HQ, CS, and SC display a spatial distribution of "high values in the northwest and low values in the southeast" (Figure 5). Areas with high values for these services are predominantly located within BS and ST. These zones are typified by expansive

natural and semi-natural forest landscapes, along with land cover primarily consisting of forest and grassland (Figure 4). Furthermore, the implementation of ecological restoration initiatives—such as the Grain for Green Program—in the BTH region has generated a notable increase in vegetation coverage across these areas. The dense vegetation canopy and structurally complex plant communities in this region enhance both carbon sequestration capacity and habitat integrity [49]. The well-developed root system effectively intercepts precipitation, exerting a strong positive effect on enhancing soil erosion resistance and runoff resistance [55]. These findings are in line with those in prior studies [5,56]. Moreover, this study found that the spatial distribution of WY exhibits a trend of decreasing values from the southeast to the northwest. Such a pattern underscores the significant influence of land-use categories, vegetation coverage, and evapotranspiration rates on WY provision. Specifically, forested areas with dense vegetation contribute substantially to water consumption through intense transpiration processes. The dense vegetation canopy also retains and evaporates a certain amount of water, resulting in high actual evapotranspiration and a reduction in local WY. In addition, croplands exhibit a lower transpiration rate compared to dense forest canopies and experience less ground evaporation than urban areas, resulting in reduced direct water loss from soil into the atmosphere. Consequently, the southeastern plains—where farmland is extensive, as in HX and TZ—show higher WY values. This pattern is also in line with findings from earlier studies [54,57].

In this research, the spatial distribution of MESLI across the BTH region demonstrates a characteristic of "high values in the northwest and low values in the southeast". This trend may be due to the extensive forest and grassland coverage in the northwestern mountainous areas, where dense vegetation and high biodiversity enhance the capacity to deliver integrated ecosystem services. In contrast, HX, TX, and BH have lower elevations and flat terrain, with towns and villages distributed widely and densely. Land-use types shift from forest and grassland to urbanland, with human activity having a stronger impact the closer one gets to built-up areas. Meanwhile, the plains are characterized by an extensive distribution of cropland. The homogeneity of vegetation types and the primary focus on grain production in these areas constrain their capacity to deliver diverse ecosystem services, which is reflected in their comparatively lower MESLI values. Furthermore, simulation results across various scenarios in this research reveal that the average MESLI under the EP scenario is greater than that in the others, indicating a greater future capacity for the provision of multiple ecosystem services in the BTH region under such conditions. This outcome is in agreement with the findings of Lin et al. [58], who also reported uniformly higher levels of ESs under ecological protection-oriented strategies.

### *4.2. Analysis of Trade-Off and Synergy Between ESs*

Ecosystem services (ESs) interact through either synergistic or trade-off relationships. A comprehensive understanding of these complex interactions is fundamental to the design of effective framework for managing ESs [59]. The findings demonstrate that the trade-offs and synergies between ESs in BTH show a high degree of stability. Specifically, a trade-off interaction exists between supply services and regulation services, while a synergistic interaction is observed between regulation services and support services. These results align with earlier studies [47,60,61]. Forests with dense vegetation often have complex vegetation structures. Tall, mature trees have natural carbon sink functions, which are conducive to the accumulation of organic carbon and create favorable conditions for animal and plant habitats. Enhanced biodiversity contributes to the long-term capacity of forests to sequester and store carbon [62], thereby establishing a pronounced synergistic effect between biodiversity and carbon accumulation. Enhanced vegetation coverage contributes to the reduction in precipitation-induced soil erosion; however, it simultaneously results

in a decline in surface water yield. Consequently, at the global scale, HQ, CS, and SC demonstrate synergistic interactions, whereas WY shows a trade-off relationship with these ESs.

A comparative analysis of ESs interactions across the entire BTH region and within its individual functional sub-regions indicates that identical ESs can manifest distinct interactive relationships depending on the main functional zone. From a regional perspective, HQ, CS, and SC services are mutually synergistic. However, in local functional zones such as HX and TZ, the correlation between SC, HQ, and CS exhibits a weak trade-off relationship (Figure 8). Meanwhile, all six paired interactions among ESs in the BH region show synergistic effects, a phenomenon potentially associated with land-use patterns and regional climatic conditions [63,64]. HX and TZ serve as the main agricultural production zones within BTH, where cropland and urbanland constitute the dominant land-use types.

The observed weak trade-off among SC, HQ, and CS in these regions fundamentally reflects underlying spatial and managerial conflicts in the supply of these ESs. Specifically, the spatial conflict manifests in the fact that the same unit of land is often utilized for intensive agriculture—where soil management practices aim to maintain SC—while also being critically needed to support natural vegetation for sustaining HQ and CS. However, in the plain areas of HX and TZ, these land units are predominantly occupied by cropland and construction land, which directly excludes the presence of forests or wetlands that are essential for maintaining high levels of HQ and CS. In terms of land-use management, conflict also arises due to divergent priorities among different land-use strategies. Agricultural management focuses on optimizing production and enhancing soil conservation, yet this often occurs at the expense of natural habitats and long-term carbon sequestration. For example, although practices such as cover cropping and terracing can improve SC, they cannot replicate the complex, multi-layered ecological structure of forests that supports HQ, nor can they provide the substantial biomass required for stable CS [65,66]. Consequently, these conditions lead to a weak trade-off relationship among SC, HQ, and CS in HX and TZ.

Prediction results under different scenarios indicate that the trade-off relationship between WY, HQ, and CS is more intense under the EC scenario than in any other scenarios. This outcome is associated with the predefined conditions of the scenario, under which a substantial expansion of construction land results in a sharp decline in natural vegetation (e.g., forests and grasslands) and semi-natural land cover (e.g., croplands). These changes significantly affect the provision of WY, HQ, and CS. Specifically, the increase in built-up areas enhances surface impermeability, which reduces rainfall infiltration and directs a larger proportion of precipitation into surface runoff, thereby considerably elevating WY. The spread of urbanland also fragments natural habitats, disrupts wildlife corridors, and diminishes the extent of suitable habitats, adversely impacting HQ and CS. The urban heat island effect and heightened pollution emissions further intensify environmental stress, resulting in a decline in HQ and CS, which in turn amplifies the trade-off relationship among WY and these services. Under the ND scenario, shifts in land utilization occur at a comparatively gradual pace, with the growth of urbanland areas remaining constrained. As a result, changes in WY, HQ, and CS remain relatively balanced, and their trade-off relationship is weak. In contrast, the EP scenario prioritizes the preservation of ecologically significant lands including forests and wetlands. The resulting increase in vegetation coverage substantially enhances both HQ and CS. Although WY may experience a slight reduction due to increased evapotranspiration following vegetation restoration, the synergy among these three ESs is strengthened, leading to the weakest trade-off relationship across all scenarios.

Moreover, when viewed within the broader context of global urbanization, the ESs trade-offs observed in the BTH region are also prevalent in the development of other

major urban agglomerations, such as the Yangtze River Delta [67] and the Pearl River Delta [16]. For instance, these regions consistently demonstrate synergistic relationships among HQ, CS, and SC. This confirms that the ESs trade-off analysis framework based on land-use simulations possesses broad applicability in studies of urban agglomerations across diverse geographical settings. However, the BTH case also reveals its unique characteristics: compared to the water-rich Yangtze River Delta and Pearl River Delta, the BTH region experiences more intense and sensitive trade-offs between WY and other ESs due to its water scarcity. Consequently, while building on its general applicability, the framework developed in this study—by incorporating functional zone-specific natural and policy constraints—provides a more tailored reference for understanding and managing ecological security issues in comparable regions.

### *4.3. Suggestions for Future Regional Planning*

Predicting and evaluating ESs under future scenarios, while examining the impact of LUCC on ESs, assists policymakers in anticipating policy outcomes and mitigating potential negative effects [68]. Furthermore, the multi-scenario simulation results of land use in this study carry significant policy implications for the ongoing "Beijing–Tianjin–Hebei Coordinated Development" and "Ecological Conservation Redline" strategies. The findings indicate that under the EP scenario, the area of regional forests and grassland is effectively maintained, which aligns closely with the core protected zones designated by the ecological redline. This suggests that the current redline policy is effective in safeguarding key ESs, such as biodiversity. However, this study also reveals that under the EC scenario, construction land substantially encroaches upon cultivated and ecological land near the redline, creating a potential risk of "protection inside the redline, but squeeze-out effects outside it." Therefore, we recommend that future regional planning should transition from simple "line-drawing" management to a multi-tiered and refined control system of "redline-buffer zone-coordinated development zone" and incorporate ESs trade-off analysis as a crucial tool for evaluating regional planning schemes.

In BTH, analyzing ESs trade-offs and synergies using functional zones as the study units can fully leverage their roles as spatial connectors and carriers, thereby facilitating the formation of a comprehensive layout characterized by functional diversity, complementary advantages, and regional coordination and thus enhancing the level of ecological environmental protection. By analyzing the proportions of the trade-offs and synergies relationship of ESs in functional zones under three scenarios for 2035 (Figure 10), the following recommendations are proposed, taking into account regional characteristics and the future development needs of each functional zone: (1) In BS and ST, a strong trade-off relationship exists between WY and both CS and SC. Due to plant transpiration, the expansion of woodland areas consumes substantial water resources, thereby reducing WY. Consequently, future development must strictly prohibit the establishment of high-density, high-water-consumption plantations (e.g., *monoculture poplar forests*) in deeply arid areas. Instead, efforts should focus on promoting the cultivation of native, drought-tolerant, and low-water-demand shrubs and herbaceous plants (such as sea buckthorn, Caragana korshinskii, and Stipa species) to establish near-natural "tree–shrub–grass" composite ecosystems. Furthermore, "enclosure and conservation" measures should be implemented for existing natural desert vegetation to minimize human disturbance. Additionally, under different future development models, the EP scenario shows a lower proportion of high trade-offs and an increased proportion of high synergies. In future development, it is essential to fully reference the development model of this scenario, restrict the conversion of ecological land, and strictly manage ecological spaces to enhance the protective and regulatory functions of the ecological barrier zone. (2) The interrelationships among ESs in

HX and TZ are primarily characterized by low synergistic relationships, indicating that the supply capacities of all four ESs in these two zones are at medium or below-medium levels. Considering the strong carbon sequestration and water retention capabilities of forest and grassland, appropriate land conversion in this region could promote the recovery of natural ecosystems and bolster the region's resilience in delivering a diverse suite of ecosystem services. Furthermore, to address the weak trade-off relationships between SC and HQ, CS, future ecological management could prioritize the conversion of low-yield farmland or degraded land—particularly on steep slopes and within key ecological corridor areas—into mixed forests. This approach would mitigate the weak trade-offs among SC, HQ, and CS, thereby achieving the goal of simultaneously enhancing the supply capacity of all three ecosystem services. Additionally, in future development, TZ could consider relocating to surrounding areas with lower elevation variations and suitable terrain for development, establishing an integrated development framework combining "ecological protection and economic development" objectives to foster regional harmonious growth. (3) BH is the core zone for opening up, industrial upgrading, and marine economy in the BTH coordinated development strategy. The interrelationship among the four ESs is primarily characterized by high trade-offs. In the three future scenarios, the proportion of strong synergy increases in the EP scenario. Therefore, in future development, the development model of this scenario can be referenced to prioritize marine ecological protection while developing port economies, strengthen coastal environmental protection and restoration, and advance the harmonious growth of economic construction and marine ecology.

### *4.4. Limitations and Further Research*

This research forecasts land-use configurations under multiple scenarios, taking into account both the comprehensive spatial planning and functional zoning of the study region. Subsequently, it examines how interactions among ESs evolve across various functional zones under each scenario. The findings offer a scientific foundation for developing policies related to regional ecosystem management. Nevertheless, several limitations should be noted: Although the PLUS model incorporates a patch-generation strategy and land-use expansion analysis, land-use prediction models generally struggle to capture the slow succession processes of future natural ecosystems and their lagged responses to land policies [69]. Meanwhile, climate change is a critical factor influencing ESs. However, due to challenges in obtaining high-resolution and reliable future climate projection data, this study did not integrate climate scenarios (e.g., RCPs/SSPs) into the comprehensive analytical framework. In future research, it would be valuable to combine top-down macroscopic prediction models with the PLUS model and incorporate machine learning approaches to uncover deeper, nonlinear characteristics of land-use change. Scenario design could also be diversified—for instance, by introducing a land-use optimization scenario under carbon neutrality constraints—to further explore LUCC patterns that align with the coordinated development of the Beijing–Tianjin–Hebei region. Additionally, while this study analyzed trade-offs and synergies among ESs in the study area primarily at the pixel scale, it is important to note that ESs relationships exhibit significant scale dependence and spatial heterogeneity [19,49]. Therefore, future studies should strive to address these limitations by integrating climate change impacts and multi-scale spatial analysis to enhance the credibility and robustness of assessment results.

## 5. Conclusions

This study adopts a dual temporal perspective encompassing historical trends and future projections. The land-use projections under different scenarios are developed by accounting for the development positioning and policy constraints of various functional

zones. This study analyzes land-use dynamics and ESs characteristics across the entire region and within functional zones, based on three scenarios projected for 2035. Furthermore, it explores the synergies and trade-offs among ESs across different functional zones, to elucidate the impact of LUCC on ESs. The key results from this research can be distilled to the following points: (1) Land-use patterns from 2020 to 2035 exhibit significant variation across the different scenarios. Within the ND scenario, urbanland areas show continued expansion, primarily encroaching on cropland and grassland. In contrast, the EP scenario demonstrates effective conservation of ecological land, including forest and grassland cover. Under the EC scenario, arable land decreases the most ($8.77 \times 10^3$ km), and construction land expands the most ($8.93 \times 10^3$ km). (2) In BTH, the provision of ESs demonstrates significant spatial variability. HQ, CS, and SC display comparable spatial patterns, generally following a trend of "high values in the northwest and low values in the southeast". In contrast, WY is characterized by a spatial pattern of "high in the southeast and low in the northwest". The characteristics of spatial patterns of MESLI under 2020 and across the three 2035 scenarios show relative consistency, with zones of elevated values predominantly found in areas of dense vegetation cover, including BS and ST. This suggests a strengthened ability of these regions to deliver a diverse suite of ESs. In comparison with the other two scenarios, the EP scenario demonstrates a more extensive distribution of high-value areas, reflecting an overall enhancement in the provision of ESs under this particular pathway. (3) In BTH, the correlation coefficients among ESs show considerable variation both at the regional scale and within individual functional zones. Furthermore, the correlation and strength between ESs vary across different functional zones depending on their type and spatial location. Similar types of services also demonstrate divergent trade-off or synergy behaviors depending on the functional zone in which they are located.

**Supplementary Materials:** The following supporting information can be downloaded at https://www.mdpi.com/article/10.3390/land14112176/s1, Table S1: Cost matrices of BS; Table S2: Cost matrices of ST; Table S3: Cost matrices of HX; Table S4: Cost matrices of TZ; Table S5: Cost matrices of BH; Table S6: Habitat quality module threat data; Table S7: Sensitivity of different land-use types to threat sources; Table S8: Carbon density values of different land-use types in the BTH region; Table S9: Biophysical table in WY; Table S10: Biophysical table in SC.

**Author Contributions:** X.H.: Conceptualization, Methodology, Visualization, Writing—original draft, Formal analysis. Y.L. (Yang Li): Conceptualization, Methodology, Project administration. W.L. and Y.L. (Yancang Li): Funding acquisition, Writing—review and editing, supervision. Z.S., N.W. and Z.L.: Software and Data processing. B.X., S.Y. and S.W.: Visualization and supervision. J.Z. and S.Z.: Formal analysis. All authors have read and agreed to the published version of the manuscript.

**Funding:** This research was funded by the National Natural Science Foundation of China (No. 42001027, 42101019); the Natural Science Foundation of Hebei Province (D2025403079, D2021403023, D2024205037); the Science and Technology Project of the Hebei Education Department (BJK2022022, BJK2024075); the Central Guidance on Local Science and Technology Development Fund of Hebei Province, China (236Z4201G); the Project for the Construction of the Natural Resources Observation Indicator System and Thematic Research in Typical Areas of the Haihe River Basin (13000025P006CA410574D); the 21st Student Research Project of Hebei GEO University (KAY202511, KBY202504); and the Special Soft Science Research Project of The Innovation Capacity Enhancement Plan of Hebei Province (25357403D).

**Data Availability Statement:** The original contributions presented in this study are included in the article/Supplementary Material. Further inquiries can be directed to the corresponding authors.

**Conflicts of Interest:** The authors declare no conflicts of interest.

## References


1. Li, J.; Bai, Y.; Alatalo, J.M. Impacts of Rural Tourism-driven Land Use Change on Ecosystems Services Provision in Erhai Lake Basin, China. *Ecosyst. Serv.* **2020**, *42*, 101081. [CrossRef]
2. Liang, X.; Jin, X.; Ren, J.; Gu, Z.; Zhou, Y. A Research Framework of Land Use Transition in Suzhou City Coupled with Land Use Structure and Landscape Multifunctionality. *Sci. Total. Environ.* **2020**, *737*, 139932. [CrossRef] [PubMed]
3. Liu, S. Effects of Landscape Pattern Change on Ecosystem Services and Its Interactions in Karst Cities: A Case Study of Guiyang City in China. *Ecol. Indic.* **2022**, *145*, 109646. [CrossRef]
4. Sun, L.; Yu, H.; Sun, M.; Wang, Y. Coupled Impacts of Climate and Land Use Changes on Regional Ecosystem Services. *J. Environ. Manag.* **2023**, *326*, 116753. [CrossRef]
5. Feng, Z.; Jin, X.; Chen, T.; Wu, J. Understanding Trade-Offs and Synergies of Ecosystem Services to Support the Decision-Making in the Beijing–Tianjin–Hebei Region. *Land Use Policy* **2021**, *106*, 105446. [CrossRef]
6. Tian, Y.; Xu, D.; Song, J.; Guo, J.; You, X.; Jiang, Y. Impacts of Land Use Changes on Ecosystem Services at Different Elevations in an Ecological Function Area, Northern China. *Ecol. Indic.* **2022**, *140*, 109003. [CrossRef]
7. Busch, M. Potentials of Quantitative and Qualitative Approaches to Assessing Ecosystem Services. *Ecol. Indic.* **2012**, *21*, 89–103. [CrossRef]
8. Zhou, Z. Experimental Research on Trade-Offs in Ecosystem Services: The Agro-Ecosystem Functional Spectrum. *Ecol. Indic.* **2019**, *106*, 105536. [CrossRef]
9. Feng, Q. Ecosystem Service Trade-Offs and Their Influencing Factors: A Case Study in the Loess Plateau of China. *Sci. Total Environ.* **2017**, *607–608*, 1250–1263. [CrossRef]
10. Li, W.; Kang, J.; Wang, Y. Effects of Habitat Fragmentation on Ecosystem Services and Their Trade-Offs in Southwest China: A Multi-Perspective Analysis. *Ecol. Indic.* **2024**, *167*, 112699. [CrossRef]
11. Liu, L. Trade-off Analyses of Multiple Mountain Ecosystem Services along Elevation, Vegetation Cover and Precipitation Gradients: A Case Study in the Taihang Mountains. *Ecol. Indic.* **2019**, *103*, 94–104. [CrossRef]
12. Wang, Z. Exploring the Interdependencies of Ecosystem Services and Social-Ecological Factors on the Loess Plateau through Network Analysis. *Sci. Total Environ.* **2025**, *960*, 178362. [CrossRef]
13. Chen, X.; Zou, C.; Zhang, Y. Spatial Flows of Ecosystem Services under Future Climate and Land-Use Changes. *Environ. Res. Lett.* **2024**, *19*, 024044. [CrossRef]
14. Zhang, Y.; Yu, P.; Tian, Y.; Chen, H.; Chen, Y. Exploring the Impact of Integrated Spatial Function Zones on Land Use Dynamics and Ecosystem Services Tradeoffs Based on a Future Land Use Simulation (FLUS) Model. *Ecol. Indic.* **2023**, *150*, 110246. [CrossRef]
15. Ran, C.; Wang, S.; Bai, X.; Tan, Q.; Zhao, C.; Luo, X.; Chen, H.; Xi, H. Trade-Offs and Synergies of Ecosystem Services in Southwestern China. *Environ. Eng. Sci.* **2020**, *37*, 669–678. [CrossRef]
16. Shao, Y.; Xiao, Y.; Sang, W. Land Use Trade-Offs and Synergies Based on Temporal and Spatial Patterns of Ecosystem Services in South China. *Ecol. Indic.* **2022**, *143*, 109335. [CrossRef]
17. Gou, M. Identifying and Analyzing Ecosystem Service Bundles and Their Socioecological Drivers in the Three Gorges Reservoir Area. *J. Clean. Prod.* **2021**, *307*, 127208. [CrossRef]
18. Wang, H.; Liu, L.; Yin, L.; Shen, J.; Li, S. Exploring the Complex Relationships and Drivers of Ecosystem Services across Different Geomorphological Types in the Beijing-Tianjin-Hebei Region, China (2000–2018). *Ecol. Indic.* **2021**, *121*, 107116. [CrossRef]
19. Zhou, J.; Zhang, B.; Zhang, Y.; Su, Y.; Chen, J.; Zhang, X. Research on the Trade-Offs and Synergies of Ecosystem Services and Their Impact Factors in the Taohe River Basin. *Sustainability* **2023**, *15*, 9689. [CrossRef]
20. Shi, M.; Wu, H.; Fan, X.; Jia, H.; Dong, T.; He, P.; Baqa, M.F.; Jiang, P. Trade-Offs and Synergies of Multiple Ecosystem Services for Different Land Use Scenarios in the Yili River Valley, China. *Sustainability* **2021**, *13*, 1577. [CrossRef]
21. Yu, P.; Zhang, S.; Yung, E.H.K.; Chan, E.H.W.; Luan, B.; Chen, Y. On the Urban Compactness to Ecosystem Services in a Rapidly Urbanising Metropolitan Area: Highlighting Scale Effects and Spatial Non–Stationary. *Environ. Impact Assess. Rev.* **2023**, *98*, 106975. [CrossRef]
22. Kalantari, Z.; Ferreira, C.S.S.; Pan, H.; Pereira, P. Nature-Based Solutions to Global Environmental Challenges. *Sci. Total Environ.* **2023**, *880*, 163227. [CrossRef] [PubMed]
23. Ma, S.; Wang, L.-J.; Zhu, D.; Zhang, J. Spatiotemporal Changes in Ecosystem Services in the Conservation Priorities of the Southern Hill and Mountain Belt, China. *Ecol. Indic.* **2021**, *122*, 107225. [CrossRef]
24. Yu, L.; Leng, G.; Tang, Q.; Lu, C.; Gao, Y.; Yao, L.; Fan, S.; Dong, J.; Tu, H.; Ai, Z.; et al. Land-Atmosphere Interactions Mitigate the Direct Surface-Drying Effects of Land Use and Cover Change. *One Earth* **2025**, *8*, 101210. [CrossRef]
25. Sun, Y.; Li, J.; Ren, Z.; Yang, F. Ecosystem Service Trade-Offs and Spatial Pattern Optimisation under Different Land Use Scenarios: A Case Study in Guanzhong Region, China. 2023, 12, 236.
26. Jingjing, Z.; Wenbo, Z.; Lianqi, Z.; Yanhong, L. Multi-Scale Analysis of Trade-off/Synergistic Effects of Forest Ecosystem Services in the Funiu Mountain Region, China. *J. Geogr. Sci.* **2022**, *32*, 981–999.

27. Wang, M. Exploring the Response of Trade-Offs and Synergies among Ecosystem Services to Future Land Use Changes in the Hilly Red Soil Region of Southern China. *J. Environ. Manag.* **2024**, *372*, 123283. [CrossRef]
28. Dong, X. Entwining Ecosystem Services, Land Use Change and Human Well-Being by Nitrogen Flows. *J. Clean. Prod.* **2021**, *308*, 127442. [CrossRef]
29. Hasan, S.S.; Zhen, L.; Miah, M.G.; Ahamed, T.; Samie, A. Impact of Land Use Change on Ecosystem Services: A Review. *Environ. Dev.* **2020**, *34*, 100527. [CrossRef]
30. Zhang, Y.; Chang, X.; Liu, Y.; Lu, Y.; Wang, Y.; Liu, Y. Urban Expansion Simulation under Constraint of Multiple Ecosystem Services (MESs) Based on Cellular Automata (CA)-Markov Model: Scenario Analysis and Policy Implications. *Land Use Policy* **2021**, *108*, 105667. [CrossRef]
31. Lei, J.; Wang, S.; Wu, J.; Wang, J.-W.; Xiong, X. Land-Use Configuration Has Significant Impacts on Water-Related Ecosystem Services. *Ecol. Eng.* **2021**, *160*, 106133. [CrossRef]
32. Li, Z.; Jiang, W.; Peng, K.; Wang, X.; Deng, Y.; Yin, X.; Ling, Z. Comparative Analysis of Land Use Change Prediction Models for Land and Fine Wetland Types: Taking the Wetland Cities Changshu and Haikou as Examples. *Landsc. Urban Plan.* **2024**, *243*, 104975. [CrossRef]
33. Girma, R.; Fürst, C.; Moges, A. Land Use Land Cover Change Modeling by Integrating Artificial Neural Network with Cellular Automata-Markov Chain Model in Gidabo River Basin, Main Ethiopian Rift. *Environ. Chall.* **2022**, *6*, 100419. [CrossRef]
34. Ma, S.; Huang, J.; Wang, X.; Fu, Y. Multi-Scenario Simulation of Low-Carbon Land Use Based on the SD-FLUS Model in Changsha, China. *Land Use Policy* **2025**, *148*, 107418. [CrossRef]
35. Yang, J.; Gong, J.; Tang, W.; Liu, C. Patch-Based Cellular Automata Model of Urban Growth Simulation: Integrating Feedback between Quantitative Composition and Spatial Configuration. *Comput. Environ. Urban Syst.* **2020**, *79*, 101402. [CrossRef]
36. Liang, X.; Guan, Q.; Clarke, K.C.; Liu, S.; Wang, B.; Yao, Y. Understanding the Drivers of Sustainable Land Expansion Using a Patch-Generating Land Use Simulation (PLUS) Model: A Case Study in Wuhan, China. *Comput. Environ. Urban Syst.* **2021**, *85*, 101569. [CrossRef]
37. Wang, Y.; Li, X.; Zhang, Q.; Li, J.; Zhou, X. Projections of Future Land Use Changes: Multiple Scenarios-Based Impacts Analysis on Ecosystem Services for Wuhan City, China. *Ecol. Indic.* **2018**, *94*, 430–445. [CrossRef]
38. Huang, J.; Tang, Z.; Liu, D.; He, J. Ecological Response to Urban Development in a Changing Socio-Economic and Climate Context_ Policy Implications for Balancing Regional Development and Habitat Conservation. *Land Use Policy* **2020**, *97*, 104772. [CrossRef]
39. Chang, B.; Chen, B.; Chen, W.; Xu, S.; He, X.; Yao, J.; Huang, Y. Analysis of Trade-off and Synergy of Ecosystem Services and Driving Forces in Urban Agglomerations in Northern China. *Ecol. Indic.* **2024**, *165*, 112210. [CrossRef]
40. Sun, X.; Wu, J.; Tang, H.; Yang, P. An Urban Hierarchy-Based Approach Integrating Ecosystem Services into Multiscale Sustainable Land Use Planning: The Case of China. *Resour. Conserv. Recycl.* **2022**, *178*, 106097. [CrossRef]
41. Yang, Y.; Zheng, H.; Kong, L.; Huang, B.; Xu, W.; Ouyang, Z. Mapping Ecosystem Services Bundles to Detect High- and Low-Value Ecosystem Services Areas for Land Use Management. *J. Clean. Prod.* **2019**, *225*, 11–17. [CrossRef]
42. Zhang, D.; Huang, Q.; He, C.; Wu, J. Impacts of Urban Expansion on Ecosystem Services in the Beijing-Tianjin-Hebei Urban Agglomeration, China: A Scenario Analysis Based on the Shared Socioeconomic Pathways. *Resour. Conserv. Recycl.* **2017**, *125*, 115–130. [CrossRef]
43. Li, Z.Z.; Hu, B.; Qin, Y.; Cheng, X. Drivers of Spatiotemporal Disparities in the Supply-Demand Budget of Ecosystem Services: A Case Study in the Beijing-Tianjin-Hebei Urban Agglomeration, China. *Front. Environ. Sci.* **2022**, *10*, 955876. [CrossRef]
44. Chen, T.; Feng, Z.; Zhao, H.; Wu, K. Identification of Ecosystem Service Bundles and Driving Factors in Beijing and Its Surrounding Areas. *Sci. Total Environ.* **2020**, *711*, 134687. [CrossRef] [PubMed]
45. Gong, S.X.; Zhang, Y.H.; Li, Y.H. Spatio-Temporal Variation and Prediction of Carbon Storage in Beijing-Tianjin-Hebei Region-A PLUS-InVEST Model Approach. *J. Arid Land Resour. Environ.* **2023**, *37*, 20–28. [CrossRef]
46. Zhang, B.; Pan, P.P.; Wang, X.Y.; Wen, J.Y.; Ren, J.X.; Liu, M.M. Multi-Scenario Simulation and Functional Relationship Analysis of Land Use Change in the Beijing-Tianjin-Hebei Region Based on GMOP-PLUS Coupling Model. *Geogr. Geogr. Inf. Sci.* **2023**, *39*, 8–16.
47. Li, Q.; Bao, Y.; Wang, Z.; Chen, X.; Lin, X. Trade-Offs and Synergies of Ecosystem Services in Karst Multi-Mountainous Cities. *Ecol. Indic.* **2024**, *159*, 111637. [CrossRef]
48. Peng, L.; Deng, W.; Huang, P.; Liu, Y. Evaluation of Multiple Ecosystem Services Landscape Index and Identification of Ecosystem Services Bundles in Sichuan Basin. *Acta Ecol. Sin.* **2021**, *41*, 9328–9340. [CrossRef]
49. Shen, J.; Li, S.; Liang, Z.; Liu, L.; Li, D.; Wu, S. Exploring the Heterogeneity and Nonlinearity of Trade-Offs and Synergies among Ecosystem Services Bundles in the Beijing-Tianjin-Hebei Urban Agglomeration. *Ecosyst. Serv.* **2020**, *43*, 101103. [CrossRef]
50. He, L.; Xie, Z.; Wu, H.; Liu, Z.; Zheng, B.; Wan, W. Exploring the Interrelations and Driving Factors among Typical Ecosystem Services in the Yangtze River Economic Belt, China. *J. Environ. Manag.* **2024**, *351*, 119794. [CrossRef]

51. Chen, Y.; Feng, X.; Fu, B.; Ma, H.; Zohner, C.M.; Crowther, T.W.; Huang, Y.; Wu, X.; Wei, F. Maps with 1 Km Resolution Reveal Increases in Above- and Belowground Forest Biomass Carbon Pools in China over the Past 20 Years. *Earth Syst. Sci. Data* **2023**, *15*, 897–910. [CrossRef]
52. Zhang, J.; Zhang, Z.; Liu, L.; Cao, Y.; Zhang, M.; Yuan, Z.; Ma, R.; Liu, X.; Liu, Y. Scaling Effects of Ecosystem Service Trade-off and Synergy in Arid Inland River Basins: A Case Study of the Manas River Basin of Xinjiang, China. *Ecol. Indic.* **2025**, *173*, 113358. [CrossRef]
53. Xu, J.; Wang, S.; Xiao, Y.; Xie, G.; Wang, Y.; Zhang, C.; Li, P.; Lei, G. Mapping the Spatiotemporal Heterogeneity of Ecosystem Service Relationships and Bundles in Ningxia, China. *J. Clean. Prod.* **2021**, *294*, 126216. [CrossRef]
54. Xu, W.; Xu, H.; Li, X.; Qiu, H.; Wang, Z. Ecosystem Services Response to Future Land Use/Cover Change (LUCC) under Multiple Scenarios: A Case Study of the Beijing-Tianjin-Hebei (BTH) Region, China. *Technol. Forecast.* **2024**, *205*, 123525.
55. Tasser, E.; Leitinger, G.; Tappeiner, U.; Schirpke, U. Shaping the European Alps Trends in Landscape Patterns, Biodiversity and Ecosystem Services. *Catena* **2024**, *235*, 107607. [CrossRef]
56. Yan, Y.; Qin, Y.W.; Dong, J.Q.; Cao, J.S.; Xiao, J.Y. Analysis on ecosystem service trade-offs/synergies and drivers in Beijing-Tianjin-Hebei region. *Acta Sci. Circumstantiae* **2025**, *45*, 493–506.
57. Dou, P.F.; Zuo, S.D.; Ren, Y.; Dai, S.Q.; Yun, G.L. The Impacts of Climate and Land Use/Land Cover Changes on Water Yield Service in Ningbo Region. *Acta Sci. Circumstantiae* **2019**, *39*, 2398–2409. [CrossRef]
58. Lin, M.Z.; Liu, H.Y.; Zhou, R.B.; Gong, J.Z. Evaluation and trade-offs of ecosystem services in Guangdong-Hong Kong-Macao Greater Bay Area under multi-scenario simulation. *Geographical Research* **2021**, *40*, 2657–2669.
59. Xia, H.; Yuan, S.; Prishchepov, A.V. Spatial-Temporal Heterogeneity of Ecosystem Service Interactions and Their Social-Ecological Drivers: Implications for Spatial Planning and Management. *Resour. Conserv. Recycl.* **2023**, *189*, 106767. [CrossRef]
60. Huang, J.; Zheng, F.; Dong, X.; Wang, X.-C. Exploring the Complex Trade-Offs and Synergies among Ecosystem Services in the Tibet Autonomous Region. *J. Clean. Prod.* **2023**, *384*, 135483. [CrossRef]
61. Wang, Y.; Dai, E. Spatial-Temporal Changes in Ecosystem Services and the Trade-off Relationship in Mountain Regions: A Case Study of Hengduan Mountain Region in Southwest China. *J. Clean. Prod.* **2020**, *264*, 121573. [CrossRef]
62. Yang, J.; Chen, Z.; Zhang, W.; Meng, G.; Cao, M.; Li, J.; Xu, C.; Wu, R.; Leng, H.; Wen, Q.; et al. Relationships among Multiple Ecosystem Services in Mountainous Regions: A Case Study of the Gaoligong Mountains. *J. Environ. Manag.* **2025**, *387*, 125765. [CrossRef]
63. Luo, R.; Yang, S.; Wang, Z.; Zhang, T.; Gao, P. Impact and Trade off Analysis of Land Use Change on Spatial Pattern of Ecosystem Services in Chishui River Basin. *Environ. Sci. Pollut. Res.* **2022**, *29*, 20234–20248. [CrossRef] [PubMed]
64. Wang, H.; Wang, W.J.; Wang, L.; Ma, S.; Liu, Z.; Zhang, W.; Zou, Y.; Jiang, M. Impacts of Future Climate and Land Use/Cover Changes on Water-Related Ecosystem Services in Changbai Mountains, Northeast China. *Front. Ecol. Evol.* **2022**, *10*, 854497. [CrossRef]
65. Zhou, Y.P.; Liu, X.; Liu, L.; Li, F.P.; Li, X.G.; Bai, Y. Spatio-Temporal Dynamics and Influencing Factors of Trade-off Intensity among Territorial Space Functions in the Beijing-Tianjin-Hebei Region (2000–2020). *Acta Ecol. Sin.* **2024**, *44*, 977–991. [CrossRef]
66. Bi, S.; Li, Z.; Chen, Y.; Zhang, Q.; Ye, T. Identification of Priority Conservation Areas in Beijing-Tianjin-Hebei Using Multi-Scenario Trade-Offs Based on Different Spatial Scales and Their Drivers. *Ecol. Indic.* **2024**, *166*, 112508. [CrossRef]
67. Yao, S.; Li, Y.; Quan, X.; Huang, G.; Xu, J. Exploring the Trade-Offs and Synergies among Ecosystem Services to Support Ecological Management in the Yangtze River Delta Urban Agglomeration. *J. Environ. Manag.* **2025**, *393*, 127028. [CrossRef]
68. Liu, J. Leveraging the Metacoupling Framework for Sustainability Science and Global Sustainable Development. *Natl. Sci. Rev.* **2023**, *10*, nwad090. [CrossRef] [PubMed]
69. Chen, G.; Li, X.; Liu, X.; Chen, Y.; Liang, X.; Leng, J.; Xu, X.; Liao, W.; Qiu, Y.; Wu, Q.; et al. Global Projections of Future Urban Land Expansion under Shared Socioeconomic Pathways. *Nat. Commun.* **2020**, *11*, 537. [CrossRef] [PubMed]


**Disclaimer/Publisher's Note:** The statements, opinions and data contained in all publications are solely those of the individual author(s) and contributor(s) and not of MDPI and/or the editor(s). MDPI and/or the editor(s) disclaim responsibility for any injury to people or property resulting from any ideas, methods, instructions or products referred to in the content.